DIFFUSION COEFFICIENTS OF HYDROLOGIC TRACERS AS MEASURED BY A TAYLOR DISPERSION APPARATUS

By PING HU

Advisors: Dr. John L. Wilson and Dr. Rob S. Bowman

Submitted in Partial Fulfillment of the Requirements for the Degree of
Master of Science in Hydrology

December 2000

New Mexico Institute of Mining and Technology
Socorro, New Mexico

Abstract

We developed an experimental system for measuring the diffusion coefficients of hydrologic tracers and other tracer solutes in aqueous solutions based on the Taylor dispersion technique. We give a detailed description of the instrument, experimental procedures, calibration, and data analysis for diffusion coefficient measurements. In order to test the accuracy of this system, we measured the diffusion coefficients of KCl, KBr, KI and benzoic acid in Type I water and found that our results agreed well with published data within an accuracy of 5 percent. We also found that the diffusion coefficient of KCl in water decreased slightly with increasing concentrations and our measured diffusion coefficients of KCl at different concentrations were within 2 percent of published data. All these results clearly demonstrated that the experimental system and methods we developed can be effectively used to measure diffusion coefficients for solutes of interest in hydrology.

Accordingly, we report the diffusion coefficients of a suite of fluorobenzoic acids (FBAs) and two chlorobenzoic acids (DCBAs) in Type I water and 0.1 M potassium phosphate buffer solution using our developed instrumentation and methods. The ranges of diffusion coefficients of these compounds in Type I water and buffer solution are 0.85×10^{-9} to $0.98 \times 10^{-9} m^2 s^{-1}$ and 0.74×10^{-9} to $0.98 \times 10^{-9} m^2 s^{-1}$, respectively. These solutes have proven to be effective hydrologic tracers. The measured diffusion coefficients of the benzoic acid derivatives in Type I water were approximately 17% greater than those calculated from

molecular structure. Also, the diffusion coefficients of these chemicals in Type I water, in which pH was reduced to 4.00-4.44 due to the dissociation of these weak acid chemicals, were consistently greater than those in potassium phosphate buffer solutions in which pH was adjusted to 7.0. The correlation of measured diffusion coefficients of FBAs and DCBAs in Type I water with either their molecular weight or acid dissociation constant were quite poor. However, in 0.1 M potassium phosphate buffer solution, the diffusion coefficients for FBAs tended to decrease with increasing molecular weight and to increase with the increasing negative-log acid dissociation constant, pK_a. In addition, we noticed that for FBAs of the same molecular weight, *e.g*, DFBA, TFBA or TeFBA, the diffusion coefficients varied markedly within the same group. Thus, the diffusion coefficients of FBAs and DCBAs are related to both the intrinsic properties of molecules (*e.g.*, molecular weight and geometrical configuration) as well as external factors (*e.g.*, temperature, pH, density and viscosity of medium).

Acknowledgements

First of all, I wish to express my sincerest appreciation to Dr. John Wilson and Dr. Rob Bowman for their invaluable guidance, assistance and encouragement throughout this thesis work. Their exceptional intelligence, scientific attitude and working enthusiasm with endless ideas and energy deeply inspired me. I also would really like to thank them for the opportunity of working in the exciting field of environmental hydrology in this prestigious hydrology program.

This work was funded by Los Alamos National Laboratory (subcontract number C45280016-3P) and Sandia National Laboratories (contract number AX-9014). I am thankful to Dr. P. W. Reimus and Dr. L.C. Meigs for their insightful discussion over the last two years.

I am indebted to Patci Mills and other secretaries at the Department of Earth and Environmental Science, Mary Watson-Finley at the Graduate Office, and Karen Schlue at the International Student Office, for their warm assistance and invaluable instruction throughout the duration of this program.

I also thank Jason Wise for his initial work of experimental design on which my current thesis work is based, for introducing me to this experimental system; and Roseanna Neupauer for her enduring help and friendship over the last two years. I also would like to thank many other graduate students, especially Daniel Dolmar, Jeoff Rawling, Graciella Rodriguez, Alana Fuierer and Michael Thompson, for their unforgettable help and interesting conversations.

Finally, I want to thank my husband, parents and brothers for their love, encouragement and complete understanding, otherwise, I might not have been able to dedicate all my time and energy to completing this enjoyable but busy graduate study over the past two years.

Table of Contents

Page

Acknowledgements.....ii

Table of Contents..... iv

List of Tables..... vi

List of Figures..... vii

List of Abbreviations.....ix

Approval Page

Chapter 1 INTRODUCTION AND BACKGROUND..... 1

1.1 Importance of Diffusion in Liquids..... 1

1.2 Measurement of Diffusion Coefficient..... 4

1.3 Motivation and Scope of This Work..... 8

Chapter 2 DIFFUSION THEORY IN LIQUIDS AND THE TAYLOR DISPERSION TECHNIQUE..... 11

2.1. General Diffusion Theory in Liquids..... 11

2.2. Taylor Dispersion Technique..... 12

Chapter 3 DEVELOPMENT OF INSTRUMENTATION AND METHODS..... 18

3.1. Chemicals.....18

3.2. Instrumentation and Experimental Procedure..... 19

3.3. Calibration..... 23

3.4. Data Analysis..... 29

3.5. Practical Considerations..... 30

Chapter 4 RESULTS AND DISCUSSION 34

4.1 Diffusion Coefficients of KCl, KBr, KI and Benzoic Acid in D.I Water 34

4.2 Diffusion Coefficient of Fluorobenzoic Acids (FBAs) and Two Dichlorobenzoic Acids (DCBAs) in Aqueous Solutions 40

Chapter 5 SUMMARY AND FUTURE WORK 50

5.1 Summary 50

5.2 Future work 52

REFERENCES 55

APPENDIX A: Raw Experimental Data 59

APPENDIX B: Typical CXTFIT2 Model Input / Output Files 63

APPENDIX C: Discrete Sampling Method 71

APPENDIX D: Flow Rate – Dependent Diffusion 81

APPENDIX E: Statistical Analysis of Variance for Raw Diffusion Coefficient Data 84

APPENDIX F: Diffusion Coefficient of two dye tracers: Uranine and Brilliant Blue FCF 93

APPENDIX G: Tube Radius Measurement 94

APPENDIX H: The Standard Calibration Curves of Tracers 98

List of Tables

Page

Table 1.1 Comparison of methods for measuring diffusion coefficients..... 6

Table 4.1 Diffusion coefficients of KCl, KI, KBr and benzoic acid in water..... 38

Table 4.2 Diffusion coefficients of KCl at different concentrations in water..... 40

Table 4.3 Diffusion coefficients of benzoic acid, fluorobenzoic acids (FBAs) and dichlorobenzoic acids (DCBA) in water and buffer solution..... 43

Table C-1 Repeatability tests for single drop samples..... 73

Table D-1 Diffusion coefficients of KCl, KBr, and KI in water at different flow rates..... 82

Table E-1 Raw diffusion coefficient data of FBAs and CFBAs in both water and a buffer solution..... 88

Table F-1 Diffusion coefficients of uranine and brilliant blue FCF in water..... 93

Table G-1 Tube radius measurements at different flow rates.....95

Table G-2 Tube radius measurements based on the gravimetric method.....97

List of Figures

Page

Figure 2.1 An ideal layout for the Taylor dispersion experiment..... 13

Figure 3.1 Illustrative diagram of sample injection valve..... 20

Figure 3.2 Experimental layout for diffusion coefficient measurements using the Taylor dispersion method..... 21

Figure 4.1 Output voltage from UV detector versus the concentration of benzoic acid in water..... 35

Figure 4.2 The dispersion profiles of KCl, KBr, KI, and benzoic acid in water.....36

Figure 4.3 Concentration profile of benzoic acid in water..... 37

Figure 4.4 The framework structure of benzoic acid and its substitution positions..... 41

Figure 4.5 Measured diffusion coefficient versus calculated diffusion coefficient of FBAs in water 45

Figure 4.6 Diffusion coefficients of FBAs in water (A) and 0.1 M potassium phosphate buffer (B) versus molecular weigh..... 48

Figure 4.7 Diffusion coefficients of FBAs in water (A) and 0.1 M potassium phosphate buffer solution (B) versus pK_a..... 49

Figure A-1 Three repeatable dispersion profiles of KCl (2 mM) in water at 0.1ml/min..... 60

Figure A-2 Two repeatable dispersion profiles of KBr (2 mM) in water at 0.1ml/min..... 60

Figure A-3 Three repeatable dispersion profiles of KI (2 mM) in water at 0.1ml/min..... 61

Figure A-4 Three repeatable dispersion profiles of benzoic acid (0.1mM) in water at 0.1ml/min..... 61

Figure A-5 Three repeatable dispersion profiles of PFBA (0.1mM) in water at 0.1ml/min..... 62

Figure A-6 Three repeatable dispersion profiles of 2,5 DFBA (0.1mM) in potassium phosphate buffer at 0.1ml/min..... 62

Figure C-1 Calibration curve for KI measured by HPLC system..... 77

Figure C-2 Discrete sampling breakthrough curve..... 78

Figure C-3 Simulated fraction collection..... 79

Figure C-4 Magnitude of Error as a function of fraction size..... 80

Figure D-1 Diffusion coefficients of KCl (A), KBr (B), and KI (C) in water versus the flow rates of injection..... 83

Figure G-1 Image tube cross-section under optical microscopy (100x1).....96

Figure H-1 Calibration curves of tracers at different wavelengths.....100

List of Abbreviations

c background concentration of the mobile phase

C solute concentration (M / L^3)

C_0 initial solute concentration

$\overline{C}$ radially averaged solute concentration at any selected plane in the mean velocity reference frame

ΔC the difference in concentration between the injected solution and the carrier stream

$\frac{\partial C}{\partial z}$ concentration gradient (M / L^3 / L)

$\frac{\partial C}{\partial t}$ change in concentration with time (M / L^3 / T)

D molecular diffusion coefficient (L^2 / T)

D^* hydrodynamic dispersion coefficient (L^2 / T)

F mass flux of solute per unit area per unit time

J_z solute flux density along the tube axis, z

J_r solute radial flux density

L tube length between the injection and detection points

pK_a negative log of the acid dissociation constant

ΔP pressure drop

Q flow rate of solution

r the radial distance measured perpendicularly to the axis of the tube with

radius, R

R tube radius

t_r retention time of solute dispersion profile

Δv the volume of the injected sample of solution

$V(r)$ velocity at different radial positions

$\overline{V}$ mean velocity of solution

$U(r)$ velocity relative to frame of reference

μ viscosity of the solution

η shear viscosity

ρ density of the solution

w ratio of the radius of the helix to that of tube

Re Reynold's number

De Dean number

Sc Schmidt number

Chapter 1

Introduction and Background

1.1 Importance of Diffusion in Liquids

"Diffusion is a slow transport process of matter by random thermal motion" (Tyrrell & Harris,1984) and thus often limits the rate of important chemical, biological, geological and environmental processes such as sorption, liquid-liquid mass transfer, heterogeneous chemical reactions, and microbiological growth. Diffusion occurs in the absence of any bulk fluid movement of the solution. If the solution is flowing, diffusion is coupled with the mechanical dispersion that is associated with fluctuating fluid velocities, causing further mixing of ions or molecules (Fetter,1999). Thus, diffusion is one of the most fundamental physicochemical processes in nature and plays a significant role in environmental engineering, and in surface water and groundwater hydrology.

Diffusion, as well as surface sorption and chemical reactions, influence the transport and fate of toxic heavy metals, organic contaminants, radionuclides, natural chemicals and hydrologic tracers in surface water and groundwater, because the transport of these chemicals intrinsically depends on the Brownian motion of the individual chemical solute molecule in the aqueous solution. For example, one source of toxic heavy metals in surface and groundwater is oxidation of metal sulfides (*e.g.*, pyrite) in mine tailings, which is believed to be controlled by the diffusion of free oxygen (Wunderly *et al.*, 1996). Organic

molecules are another major source of contaminants in groundwater. Biodegradation, which has been shown to be effective in remediation of organic contaminants in groundwater, depends on the diffusion of nutrients and electron acceptors (Zhang *et al.*, 1998). Intergranular diffusion of chemicals often controls the rate-limited sorption of chemicals observed in laboratory and field studies involving sediments in aquifers, vadose zones, streams and lakes. At a larger scale, especially in aquifers, diffusion into and out of lenses and layers of low permeability material plays the same role, albeit with a much longer time constant (Wilson & Bowman, 1997).

Diffusion plays a significant role in the safe storage and/or effective remediation of nuclear wastes produced by mining, industry and especially the nuclear weapons programs. There are tons of low-level and high-level nuclear wastes in Department of Energy (DOE) facilities alone. To dispose of these nuclear wastes has become a major and urgent mission of DOE and its affiliated national laboratories. The Waste Isolation Pilot Plant (WIPP) has been established in Carlsbad, New Mexico, in order to process and immobilize low-level nuclear wastes from weapons-related work. Yucca Mountain, Nevada, has been chosen as a possible repository for permanent disposal of high-level civilian nuclear wastes. Both facilities' sites are based on their unique geographical (relatively remote and low population), geological (thick salt beds at WIPP and volcanic tuff layers sandwiched between thick shale layers beneath a zeolite-dominant barrier layer upward at Yucca Mountain) and climatic (relatively dry and low rainfall) characteristics. The geology, mineralogy, petrology,

geochemistry and hydrology of the Yucca Mountain site have been extensively investigated, as has the WIPP site(*e.g.*, Bolivar *et al.*, 1990; Levy, 1991; Bish & Aronson, 1993). An important aspect of the WIPP and Yucca Mountain Site Characterization Projects is to investigate and model the flow and transport of underground water and associated radionuclides in order to ensure that the nuclear wastes can be stored permanently. Diffusion is an important process in fluid transport.

Los Alamos National Laboratory (LANL) and Sandia National Laboratories are currently responsible for hydrologic tracer tests for studying flow, transport, and fate of radionuclides under saturated conditions in the fractured tuffs near Yucca Mountain, Nevada and in fractured carbonate rocks near the WIPP site in New Mexico. Testing with conservative solute tracers (*i.e.*, tracers that do not sorb or react in any way with the surrounding rocks) is expected to yield information on water flow and fate of radionuclides through the saturated zone. Halides, fluorobenzoates, and dichlorobenzoates are normally considered as nonreactive tracers in soil and groundwater. The use of added chemical tracers allows source control and generally provides the most accurate estimates of hydrological parameters.

Because of diffusion, the tracers will not necessarily remain in mobile water in these fractured systems. Instead, they will be free to diffuse out of the fractures and into the stagnant water in the pores of the tuff or carbonate matrix, a process known as matrix diffuison (Reimus, 1996). Because the fractures are very narrow (<1 mm at Yucca Mountain), conservative solutes are expected to

have ample opportunity to diffuse into the matrix during their migration through the saturated zone. Thus, diffusion is believed to play an important role in the flow and transport of aqueous solutes. Diffusion coefficients of solutes are a basic parameter needed to evaluate transport processes, especially the propensity for radionuclides to diffuse into the matrix during their migration through the saturated zone. The diffusion coefficients for many of the tracers used at Yucca Mountain and the WIPP site have not been determined experimentally. They have only been estimated from theoretical models.

1.2 Measurement of Diffusion Coefficient

It is arguable whether the measurement of diffusion coefficient is difficult or not. On one hand, diffusion coefficients can usually be determined to within ~10% accuracy without excessive effort (Tyrrell & Harris,1984). On the other hand, such accuracy is not sufficient for some situations and improvement of instrumentation and methods is required, significantly increasing effort and expense. When developing methods for measuring diffusion coefficients, we first need to ensure that the developed methods can be effectively applied to measure the diffusion coefficients for the systems of interest and that they provide accuracy sufficient for the specific purposes. Second, we also need to ensure that the construction of the instrument is relatively inexpensive, and that the operation of the apparatus is easy.

The basic characteristics (nature of diffusion, apparatus expense, ease of apparatus construction and use, concentration difference required and method of

data collection) of some methods for measuring diffusion coefficients are compared in Table 1.1 (Cussler,1997). The first three methods (diaphragm cell, infinite couple and Taylor dispersion) in the table are most frequently used, because they are inexpensive to construct, easy to operate, and sufficiently accurate for most practical purposes. The next four methods (nuclear magnetic resonance, dynamic light scattering, Gouy and Rayleigh interferometers) in the table are generally expensive and are relatively difficult to use, but offer some advantages for the specific systems of interest. For example, dynamic light scattering is good for polymer systems; and the Rayleigh interferometer is the best method to measure concentration-dependent diffusion. The last three methods (capillary methods, spinning disk, and steady-state methods) in the table are generally inexpensive and easy to use, but require large concentration differences for measurements.

The Taylor dispersion technique may be the most commonly used technique and is considered to be the most effective for dilute solutions. It has been successfully applied in previous studies to determine diffusion coefficients for a wide range of systems including binary (*e.g.*, Taylor, 1953; Taylor, 1954, Bello *et al.,* 1994) and multicomponent solutions (*e.g.*, Leaist, 1990; Hao, 1996; Wisnudel & Torkelson, 1996; Yang & Matthews, 2000). This technique is rapid, convenient, and capable of achieving a good accuracy (*e.g.*, 1-2% error for diffusion coefficients) according to Tyrrell and Harris (1984). Because the diffusion occurs in a fine-bore tube, Taylor dispersion measurement eliminates errors from gravitational instability. This method can be used even for systems in

Table 1.1 Comparison of methods for measuring diffusion coefficients (From p 130, Cussler, 1997)

Method	Nature of diffusion	Apparatus Expense	Apparatus Construc-tion	Concent-ration difference required	Method of obtaining data	Overall value
Diaphragm cell	Pseudo-steady State	Small	Easy	Large	Concentration at known time; require chemical analysis	Excellent; simple, but occasionally erratic
Infinite couple	Unsteady in an infinite slab	Small	Easy	Large	Concentration vs. position at known time; require chemical analysis	Excellent, but restricted to solids
Taylor dispersion	Decay of a pulse	Moderate	Easy	Average	Absorbency or Refractive- index vs. time at known position	Excellent for dilute solution
Nuclear magnetic resonance	Decay of a pulse	Large	Difficult	None	Change in nuclear spin	Very good; works when other methods do not
Dynamic light scattering	Decay of a pulse	Large	Difficult	None	Doppler shift in scattered light	Very good for polymers
Gouy interfero-meter	Unsteady in an infinite cell	Large	Moderate	Small	Refractive-index gradient vs. position and time is photographed	Very good; excellect data at great effort
Rayleigh interfero-meter	Unsteady in an infinite cell	Large	Difficult	Small	Refractive index vs. position and time is photographed	Very good; best for concentration-dependent diffusion
Capillary method	Unsteady out of finite cell	Small	Easy	Average	Concentration vs. time; usually requires radioactive counter	Very good; but commonly used only with radioactive tracers
Spinning disc	Dissolution of solid or liquid	Small	Easy	Large	Concentration vs. time; requires chemical analysis	Good; requires diffusion controlled dissolution, a stringent restraint
Steady – state methods	Steady rate across known length	Moderate	Moderate	Large	Small concentration changes require exception analysis	Fair; easy analysis does not compensate for very difficult experiment

which the diffusion coefficient is low and other methods cannot be applied (Tyrrell & Harris, 1984; Schramke,1999). It is also used to study solute – solvent interaction, solute aggregation, and solute partitioning into macromolecular systems, and to assess nanoparticle sizes (Loh,1997)

1.3 Motivation and Scope of This Work

Despite the importance of diffusion to transport processes in natural and engineered systems, there is a surprising lack of direct measurements of diffusion coefficients for chemicals of significant environmental interest. It is possible to find fairly good information on diffusion coefficients for common ionic inorganic species, some information for simple organic compounds, and much less about more complex or less common organic compounds; however, nothing can be found at all on the diffusion coefficients of a number of toxic heavy metals or environmental tracers in aqueous solution. This impression is supported by searching for the diffusion coefficients in the standard reference book, the CRC Handbook of Chemistry & Physics (Lide, 1992), and confirmed by a recent monograph entitled "DNAPL Site Evaluation" by Cohen and Mercer (1993). For example, this monograph on Dense Non-Aqueous Phase Liquids (DNAPLs) contains 13 pages of property tables on organic liquids that have densities greater than water. Aqueous phase diffusion coefficients are listed for less than one fourth of these. Measured diffusion coefficients are also lacking for most organic groundwater tracers including the fluorobenzoates and the CFC's (Noulty & Leaist, 1987). Alternatively, investigators resort to calculations using empirical and theoretical relationships (Othmer & Thaker, 1953; Wilke & Chang, 1955; Duda *et al.*,1982; Lyman *et al.*, 1984; Espinosa 1987; Schramke *et al.*, 1999).

Due to the lack of direct measurements of diffusion coefficients of hydrologic tracers, and as a part of the Yucca Mountain Site Characterization Project and the WIPP Project, Los Alamos and Sandia National Laboratories

initially funded this work for the development of new methods for measuring the diffusion coefficients of tracers in hydrologic systems of interest to them. The purpose of this work was to develop an experimental system based upon the Taylor dispersion technique for measuring the diffusion coefficients of hydrologic tracers. We used alkali metal halides and suites of conservative fluorinated benzoic acids (FBAs) and dichlorinated benzoic acids (DCBAs) as tracers during the experiment. We completed experimental design and testing both for continuous and discrete sampling. The discrete sampling was required for high ionic strength solutions (details are described in Appendix C). We measured diffusion coefficients for 18 tracers in low ionic strength solutions using continuous sampling. These data should help the development and testing of conceptual models of flow and radionuclide transport over large scales in the fracture–dominated flow of the saturated zones at Yucca Mountain and the WIPP site.

The basic layout of this thesis is as follows. Chapter 1 (this chapter) gives a brief introduction on the importance of diffusion phenomena, the status of methods for measuring diffusion coefficients, and the motivations and scope of this work. A brief description of diffusion theory in liquids and the Taylor dispersion technique is given in Chapter 2. The chemicals used in this work, experimental instrumentation and its development, procedures for data collection, and models for data analysis are described in Chapter 3. To examine the wider applicability of the instrumentation system, validation of the method that we developed is also discussed in Chapter 3. Chapter 4 deals with measuring

the diffusion coefficients of 18 FBAs and DCBAs and halides in pure water and a buffer solution of 0.1 M potassium phosphate. Finally, a summary of this thesis work is given in Chapter 5. Problems we encountered and the future work we suggest are also presented in this chapter.

Chapter 2

Diffusion Theory in Liquids and The Taylor Dispersion Technique

2.1. General Diffusion Theory in Liquids

A solute in water will move from an area of greater concentration toward an area where it is less concentrated. This process is known as molecular diffusion, or diffusion (Fetter,1999). Diffusion will occur as long as a concentration gradient exists, even if the fluid is not moving. The mass flux of a diffusing fluid is proportional to the concentration gradient, which can be expressed as Fick's first law. In one dimension, Fick's first law is

$$F = -D(\partial C / \partial z) \qquad (2.1)$$

where F is the mass flux of solute per unit area per unit time; D is the molecular diffusion coefficient (L^2/T); C is the solute concentration (M/L^3); z is the distance (L); and $\frac{\partial C}{\partial z}$ is the concentration gradient ($M/L^3/L$). The negative sign indicates that the movement is from areas of greater concentration to those of lesser concentration. For systems where the concentrations are changing with time, Fick's second law applies. In one dimension this is:

$$\frac{\partial C}{\partial t} = D\frac{\partial^2 C}{\partial z^2} \qquad (2.2)$$

where $\partial C / \partial t$ is the change in concentration with time ($M/L^3/T$). The value of D in this equation can be obtained using the Taylor experimental method, which we describe below.

2.2. The Taylor Dispersion Technique

As reviewed in Cussler (1997), Griffiths first observed that when a pulse of dye solution is injected into a slow stream of solvent confined with a narrow bore tube, the resulting patch of color is found to move along the tube as a symmetrical column of slowly increasing length. This observation is in an apparent conflict with the fact that for a liquid in laminar flow through a tube, there is a parabolic distribution of velocities over any cross section normal to the tube axis. With the fluid at the center of the cross section moving at twice the average fluid velocity, fluid flow alone should distort the patch of color into a parabolic form. This discrepancy between Griffiths' observation and the parabolic velocity profile was not understood until 1953. Taylor (1953) explained that mass transport by the bulk flow of liquid through the tube is supplemented by diffusion, both along and perpendicular to the tube axis. Diffusion along the tube axis is unimportant in comparison with bulk transport, but the diffusion perpendicular to the tube axis has been shown by Taylor (1954) and Aris (1956) to be responsible for the dispersion phenomena described by Griffiths. They have shown that if certain conditions are fulfilled, the concentration distribution within the solute

column as it passes down the tube can be used to determine the inter-diffusion coefficient of a two - component system.

The Taylor dispersion technique has been successfully employed in previous studies to determine diffusion coefficients for a wide range of systems, including binary and multi-component solutions. In a Taylor diffusion experiment (Figure 2.1), a pulse of solution is injected into a carrier solution of different composition (mobile phase) flowing in a long capillary tube. Diffusion coefficients are calculated from the absorbency – index profiles across the dispersed sample peaks at or near the tube outlet.

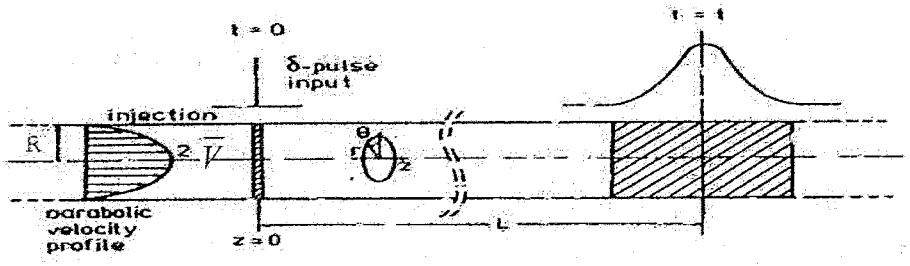

Figure 2.1 An ideal Layout for the Taylor dispersion experiment (After Alizadeh *et al.*, 1980)

The following analysis for Taylor dispersion begins with three assumptions (Cussler,1997):

(1) The injected solution is dilute. This is assumed true even for the initial pulse.

(2) The laminar flow is unchanged by the pulse. This means that the velocity varies only with radius.

(3) Mass transport is by radial diffusion and axial convection. Other transport mechanisms are negligible.

The most important assumption is the last one, because it separates diffusion and convection. It is accurate if (Aris, 1956):

$$7.2(\frac{LD}{R^2\overline{V}}) >> 1 \qquad (2.3)$$

where L is the tube length between the injection and detection, R is the tube radius and $\overline{V}$ is the mean velocity of solution (Cussler,1997). For Taylor's conditions to be met, slow flows in long tubes and/or narrow bore capillaries are required. For example, Bello *et al.* (1994) approached the problem using 50-m long by 100-μm ID (inner diameter) capillaries commonly used for capillary electrophoresis.

The most convenient arrangement to consider Taylor dispersion theoretically is to introduce a δ-pulse of a solution into a mobile phase, flowing in a straight tube (Figure 2.1). Tyrrell and Harris (1984) described that the injected pulse is carried along with an axial velocity $V(r)$, where r is the radial distance measured perpendicularly to the axis of the tube with radius R. The average velocity, $\overline{V}$ is equal to half of the maximum velocity $V(r=0)$, and $V(r)$ is given by

$$V(r) = 2\overline{V}(1-d^2) \qquad (2.4)$$

where $d = r/R$ and the velocity is measured relative to the tube. It is also convenient to measure the concentration distribution $C(z,r,t)$ relative to an axial

co-ordinate z, which moves with the mean fluid velocity $\overline{V}$. The axial flow velocity relative to this new frame of reference, $U(r)$, is from equation (2.4)

$$U(r) = V(r) - \overline{V} = \overline{V}(1 - 2d^2) \qquad (2.5)$$

The solute flux density, J_z, along the tube axis, z, relative to this reference frame, is made up of a diffusive term and a convective term

$$J_z = -D(\partial C / \partial z) + C\overline{V}(1 - 2d^2). \qquad (2.6)$$

The radial flux density, solely diffusive, is given by

$$J_r = -D(\partial C / \partial r) = -DR^{-1}(\partial C / \partial d). \qquad (2.7)$$

The concentration distribution is symmetrical about the tube axis, and the correct form for the diffusion law, analogous to equation (2.1), can be found by considering the rate of accumulation of solute in a ring-shaped element with an annular volume of inner radius r, outer radius $(r + \partial r)$, and the thickness ∂z. Application of equations (2.6) and (2.7) to the rate at which solute enters and leaves this ring by mass transport along the z and r axes, with the assumptions that diffusion is isotropic and that D is independent of concentration, gives (Tyrrell & Harris,1984)

$$\frac{\partial^2 C}{\partial d^2} + \frac{1}{d}\frac{\partial C}{\partial d} + R^2\frac{\partial^2 C}{\partial z^2} = \frac{R^2}{D}\frac{\partial C}{\partial t} + \frac{R^2 V}{D}(1 - 2d^2)\frac{\partial C}{\partial z} \qquad (2.8)$$

The operator $\partial / \partial t$ is taken at constant z, that is, at planes fixed in a reference frame moving relative to the tube with the velocity $\overline{V}$. The term $\frac{\partial^2 C}{\partial z^2}$ represents axial transport by diffusion, and Taylor has shown that this can be neglected based on assumption (3).The diffusion equation (2.8) then reduces to

$$\frac{\partial^2 C}{\partial d^2}+\frac{1}{d}\frac{\partial C}{\partial d}=\frac{R^2}{D}\frac{\partial C}{\partial t}+\frac{R^2 V}{D}(1-2d^2)\frac{\partial C}{\partial z}\ . \qquad (2.9)$$

The simplest parameter to measure experimentally is the radially- averaged solute concentration, $\overline{C}$, at any selected plane in the mean velocity reference frame. This is defined by

$$\overline{C}=2\int_0^1 C(d)\,\mathrm{d}d \qquad (2.10)$$

Taylor (1954) and Aris (1956) have shown that the dispersion process is governed by the equation

$$\frac{\partial \overline{C}}{\partial t}+\overline{V}\frac{\partial \overline{C}}{\partial Z}=D^*\frac{\partial^2 \overline{C}}{\partial z^2} \qquad (2.11)$$

if average concentration $\overline{C}$ is observed far enough down the column (equation (2.3), where D^* is a dispersion coefficient (L^2/ T). This is identical in form with equation (2.2), or Fick 's second law.

Aris (1956) showed that the dispersion coefficient is given by

$$D^*=D+\frac{R^2\overline{V}^2}{48D} \qquad (2.12)$$

For liquid-phase diffusion, the term $\frac{R^2\overline{V}^2}{48D}$ is usually several orders of magnitude larger than D, and hence

$$D^*\approx\frac{R^2\overline{V}^2}{48D} \qquad (2.13)$$

Applying the initial and boundary conditions:

$$\overline{C}(z,0)=0 \qquad (2.14)$$

$$(-D^* \frac{\partial \overline{C}}{\partial z} + \overline{V}\overline{C})_{z=0} = \overline{V}\overline{C}_0 \qquad (2.15)$$

$$\overline{C}(\infty, t) = 0 \qquad (2.16)$$

where $\overline{C}_0$ is the initial concentration of injected solution, equation (2.11) can be solved to give the radially-averaged concentration of the dispersed substance at the tube outlet, a distance L downstream from the point of injection (Hao,1996)

$$\overline{C}(t) = c + \frac{\Delta C \Delta v}{\pi R^3 \overline{V}} \sqrt{\frac{R^2 \overline{V}^2}{4D^* \pi t}} \exp\left[-\frac{R^2 \overline{V}^2 (t - t_r)^2}{4D^* r^2 t} \right] \qquad (2.16)$$

where t_r is the retention time defined by $t_r = L/\overline{V}$; Δv the volume of the injected sample of solution; ΔC the difference in concentration between the injected solution and the mobile phase and c the background concentration of the mobile phase. In this thesis, the dispersion coefficient D^* was determined from observed values of $\overline{C}(t)$ by using an iterative non-linear least-squares to fit this equation to the detected concentration. We employed the CXTFIT2 deterministic equilibrium model (MODE 1 of CXTFIT2) (Toride *et al.*, 1995) to process the experimental data for calculating the dispersion coefficient, which will be described in Chapter 3. Once the dispersion coefficient is estimated, equation (2.13) can be used to solve for the diffusion coefficient.

Chapter 3

Instrumentation and Methods

In this chapter, the procedure is described for the rapid determination of diffusion coefficients using Taylor dispersion theory. Diffusion coefficients can be determined within 5 percent accuracy (based on reference values) by carefully developing and designing the experimental instrument and method.

3.1 Chemicals

Typical chemical tracer samples (alkali metal halides, benzoic acid, fluorobenzoates and dichlorobenzoates) were used as received from both Sandia National Laboratories and Aldrich (among these tracers, only 2,3,6 TFBA; 3,4,5 TFBA and 2,3,5,6 TeFBA were received from Aldrich; the stated purity was > 99%). The solute concentrations in the injected solution were 2 mM for alkali metal halides and 0.1 mM for organic compounds. We considered higher concentration for halides because of detection limit.

The mobile phase was Type I water from a Milli-Q system for alkali metal halides. Both Type I water and 0.1 M potassium phosphate buffer solution (pH adjusted to 6.95 ± 0.02, with 44% KH_2PO_4: 56% K_2HPO_4(v/v)) were used as the mobile phases for the organic compounds. Type I water and calibrated

volumetric flasks were used to prepare the solutions. Each solution was then degassed by vacuum filtration before being loaded into the experimental system.

3.2 Instrumentation and Experimental Procedure

The apparatus for measuring diffusion coefficients was built from standard high pressure liquid chromatography (HPLC) equipment available in our laboratory. A schematic diagram of the experimental equipment is shown in Figure 3.1. A fused silica capillary tube (Polymicro Technologies, product number TSG250350), which was 2185 $\pm$1 cm long with an approximate 244 $\pm$ 6 μm internal diameter, was used in this work. The tube was wound in the form of a helix on a glass spool with a radius of 6 cm, then placed in a temperature–controlled water bath (VWR scientific Model 1186) in which temperature was kept constant (25 $\pm$ 0.1 ^{o}C). A syringe pump (ISCO model 100 DM) was used to maintain a steady flow of the mobile phase through the tube. At the beginning of each run, a narrow pulse of sample solution was loaded into the 4.9 $\pm$ 0.1 μl sample loop via an injection switching valve (Valco model C2-1026), using a syringe pump (Harvard Apparatus model 44; syringe size of 10 ml). The sample loop volume was less than 1% of the diffusion tube's internal volume. The sample valve (Figure 3.2) had 6 ports: the specific sample input in line went to port #1, sample waste went to #2, mobile phase was in #4, port #5 went to the capillary tube and detector, and the sample loop was across both ports #3 and #6. Water from the water bath was also circulated through a jacket in the ISCO pump to control mobile phase temperature.

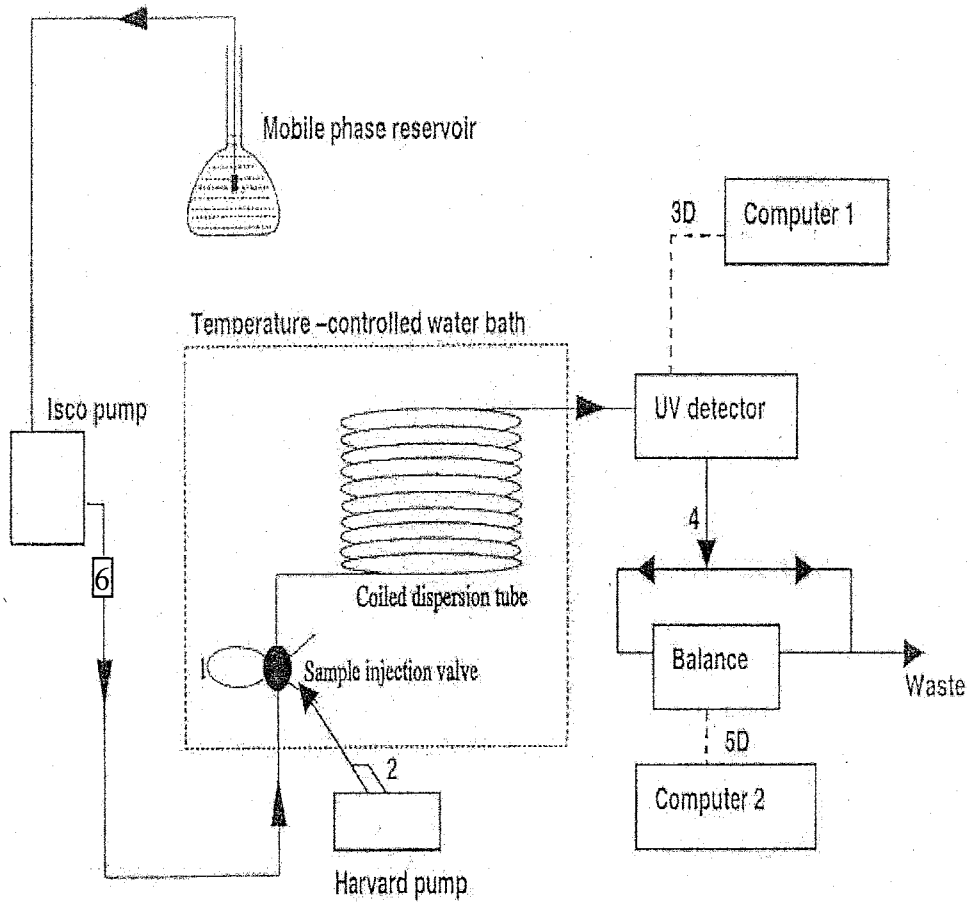

Figure 3.1 Experimental layout for diffusion coefficient measurements using the Taylor dispersion method

1. Sample loop
2. Syringe for loading sample loop
3D. Absorbance voltage data sent to Computer 1
4. Output effluent drops either go to the waste bottle or weighing by a digital balance
5D. Drop weight data sent to Computer 2.
6. Back-pressure valve

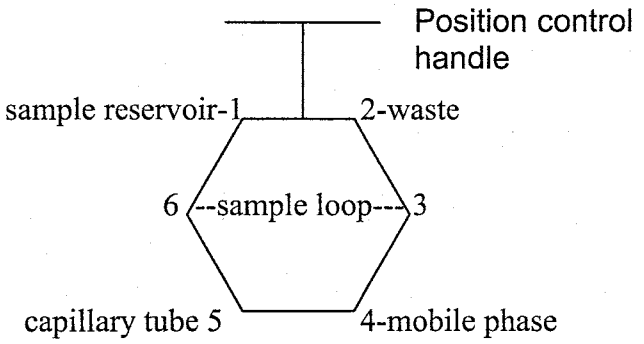

Figure 3.2 Illustrative diagram of sample injection valve

In the load position, the sample loop was filled with the appropriate tracer solution. The sample valve was switched manually for injection and that this was zero time for the experiment. The data was recorded since the sample valve was switched. When we manually switched the sample valve, the mobile phase flowed through the sample loop, carrying the sample through the coiled capillary tube to the online variable wavelength capillary detector (Thermo Seperation Products, Spectra 100 variable UV/VIS detector). Where the capillary tube passed through the window of the UV detector, the polyomid film coating the tube had been removed, exposing the tube cross section to the detector. When the dispersed samples flowed past this part of the tube, the UV detector and its computer recorded the absorbence of solute passing the tube. The output readings (voltage vs. time) were stored in the computer for subsequent numerical analysis. Details can be viewed in Appendix A. Finally, the weight of effluent drops at the end of the tube were continuously recorded at accurate time

intervals by a digital analytical balance (Mettler Type AT400) and transferred to a second computer. This data monitor was used to monitor the mobile phase flow rate using Labview (Version 6.0). The recorded data were also used to verify that the pump was running at a constant flow rate.

Before each set of experiments was run, the capillary tube and the detector were flushed with 100 ml of Type I water. Once the UV detector was warmed up for 1 hour and the baseline became stable, diffusion samples were injected every 0.5 - 1 hour. The mean liquid discharge rate was typically 0.1 ml/min, which gave the injected solute an average column residence time of about 20 min. Different detection wavelengths were used for different compounds in order to maximize sensitivity.

We selected a fused silica capillary tube for the dispersion experiment, since it had the smoothest internal surface and the most uniform diameter of the materials considered. The tube does not suffer chemically specific solute–wall interactions with the solutes we evaluated. The manufacturer of the fused silica tube also provided the maximum working pressures for the capillary tube. A back-pressure valve was inserted between the pump and the injection valve in order to control the back pressure in the pump, as it operated best at reasonably high back pressures. Among a number of available injection instruments, we chose the low volume, six-port injection valve from Valco Instruments Co. since its specification indicated the most consistent injection volume and the smallest amount of apparatus induced dispersion.

3.3 Calibration

Since the magnitude of the diffusion coefficients were very small, the experimental equipment required for data collection and experimental parameters for calculating the diffusion coefficients had to be calibrated very carefully. Our calibration was done over a range of conditions because sufficient accuracy was required for each measurement.

A number of restrictions and corrections to the analysis relating to the sample injection volume, tube radius, detector response, tube uniformity, and tube helix effects, etc., can be applied, as reviewed by Alizadeh *et al* (1980) and Tyrrell *et al* (1984).

Injection volume

The injection volume is an important parameter in estimating the solute injection time, which is an input parameter for the CXTFIT2 model, as well as injection mass. According to factory specifications, the sample loop volume was 5 μl. Since this volume was important to our calculations, we required a more accurate measurement.

We measured the sample loop volume by measuring the output effluent mass for each run. We assumed that this effluent mass was equal to the injection mass. We calculated the output effluent mass by integrating the output effluent breakthrough curve (concentration vs. time). Normalizing this result by the input concentration, we obtained an estimate for the injection or sample loop volume.

Using measurements from 20 experiments with different compounds, we calculated an injection volume of $4.85 \pm 0.11\mu l$, which we round off to $4.9 \pm 0.1\mu l$.

In addition, we determined the volume of the sample injection loop by injecting a known concentration of solute (KI) and collecting the effluent during the entire dispersion profile. We then diluted the effluent to a known volume and determined the concentration using HPLC (high performance liquid chromatography). By this method we found that our nominal 5 μl sample loop has an actual volume of $5.17 \pm 0.01\mu l$. However, we believe that HPLC method provides less accurate estimate because of more measurement error resulting from detector of HPLC.

Tube radius

The value of tube radius is critically important for estimating the diffusion coefficient by equation (2.13). The manufacturer's specifications suggested that the capillary tube radius was 125 ± 6 μm. We estimated the tube radius using three independent methods: a pressure-differential method, a microscopy method, and a gravimetric method. Details can be viewed in Appendix G.

In the pressure–differential method, we installed a differential pressure transducer at the beginning of the diffusion tube and used the pressure transducer to record the maximum pressure drop. The pressure at the end of the tube was assumed to be atmospheric (capillary effects during the formation of

drops was negligible). By Poiseuille's Law, the flow rate through a capillary in terms of pressure drop, ΔP, is given by:

$$Q = \frac{\pi R^4}{8} \frac{1}{\mu} \frac{\Delta P}{L} \qquad (3.1)$$

where Q is the flow rate of solution and μ is the viscosity of the solution. The average tube radius was calculated to be 122 ± 3 μm for several different flow rates and repeated measurements.

In the optical method, we randomly cut the capillary tube and observed its cross-sectional area under optical microscopy. The tube radius was measured by the Scion Image software program, and estimated to be 120 ± 3 μm. This method was not really accurate because the shape of the tube was altered by hand cutting.

In the gravimetric method, we randomly selected tubes of different lengths and weighed each tube when it was empty and when filled with mercury of known density. We determined the mass of mercury in the tube by weighing, and then converted that to volume of mercury and then to the tube radius. The average tube radius was determined to be 124 ± 1 μm. This method was more accurate than the optical method. However, the longest tube for measurements using this method was 1 meter. This result does not necessarily represent the average radius of the 2185 cm long tube used in the experiment.

The values for the tube radius measured by the above three methods were in good agreement, and were also close to the radius (125 ± 6 μm) of this small bore capillary tube cited by the manufacturer. However, we believe that the

pressure-differential method provides the most accurate estimate because it represents the average tube radius of the entire tube used in the experiments, while the others do not. We used this result (tube radius =122 ± 3 μm) to calculate the diffusion coefficient based on equation (2.13).

Tube length

The capillary tube length represents the travel distance of the tracers during the diffusion process. In order to accurately determine the tube length used for the experiment, we machined an aluminum cylinder with the accurate circumference of 630.56 mm. We measured the length of the tube three times by coiling it on the helix surface and counting the number of coils. The length of the diffusion tube used in the experimental system was 2185 ± 1 cm.

Flow rate

The value of flow rate is important for estimating the solute injection time. The pump was set to maintain a steady flow of the mobile phase at 0.1 ml/min. However, we found it important to verify whether or not the pump was running at a constant flow rate. The system flow rate was monitored by weighing output effluent drops over time throughout the entire experimental period, when the pump was set to a rate of 0.1 ml/min. The actual flow rate measured was 0.097 ± 0.002 ml/min. The flow rate was measured for each run for estimating the solute injection time for CXTFIT2 model. In theory, the diffusion coefficient should not vary with different flow rates. However, the diffusion coefficients measured in

our experimental system did change somewhat, when the flow rate was changed to a different value. Appendix D provides details regarding this issue. The velocity of solute was calibrated again by CXTFIT2 modeling based on the dispersion profile.

Detector response

The detector should respond linearly to the solute concentration up to some saturation concentration. We checked the detector sensitivity by injecting solute at different flow rates, and measured the concentration (as voltage) passing through the detector. The voltage readings from the detector remained the same for different flow rates using the same concentration sample.

A standard calibration curve was made for some tracers. Details can be viewed in Appendix H. We found the best linear correlation between the voltage reading and the concentration for relatively low concentrations. The calibration standards were prepared from the bulk chemicals used for those tracer injection samples. The calibration standards were also frequently analyzed to ensure that the instrumental response did not drift throughout the period of analysis. This measurement was used to assure consistent detector response throughout the analysis period and precise calibration curves for tracers on different runs.

Temperature Control

Temperature control is very important for diffusion experiments. It effects fluid viscosity and tracer diffusion coefficients, as well as the electronic output of the detector and flow meter. Since it was difficult to place all the equipment in

one temperature-controlled unit, we ensured instead that the temperature of the entire flowing pathway of the mobile phase remained constant. We inserted the capillary tube and sample injection loop in a temperature controlled water bath to maintain constant temperature (approximately 30 cm of capillary tube between the water bath and the detector had no temperature control). We placed four thermometers in the temperature-controlled water bath to measure temperature at each corner of the water bath. The average temperature measured was 25 ± 0.1 °C, when the water bath showed the reading as 25 °C. The approximate room temperature was 25 °C. We also connected the water bath to a water jacket on the ISCO pump by a plastic tube. Water circulation in the tube ensured that the mobile phase in the loop of the ISCO pump was at 25 °C before reaching the diffusion tube.

The detector was warmed up for over 1 hour prior to measurements to ensure the constant temperature of the detector assembly and to minimize the noise of voltage signals.

Balance

Standard weights (certificate number: SN 20322906, calibrated in April, 99 and expiring in April 2001) from Los Alamos National Lab were used to calibrate the balance each time before weighing the chemicals. A company (Analytical and Precision Balance, Inc) calibrated the second digital analytical balance that monitored the flow rate in Dec. 1999 before we ran the experiment. During the

experiments we periodically re-calibrated the balance using its self-calibration feature.

3.4 Data Analysis

The theoretical and mathematical description of the Taylor dispersion of a pulse of soluble substance in a solvent has been given in Chapter 2.
In our apparatus, the detector signal was sent to a computer (equipped with ChromPerfect, version 2.1) which logged the raw data as a record of voltage over time (about once per second). Calibration curves demonstrated that the voltage (the analog signal) was linearly proportional to solute concentration up to a certain concentration. The voltage was used to calculate the mean concentration of the solute passing through the detection point, based on the calibration standard curve. The dispersion coefficient was calculated from the concentration profile generated by the solute dispersion curve using the CXTFIT2 model.

One practical problem, which we often encountered, was the minor drift of baseline and starting negative voltage readings. Normalized concentration profiles were obtained by subtracting the baseline $y_0 + y_1 t$ from the raw detected concentration profile, where y_0 is the intercept of baseline and y_1 is the slope of baseline.

The corrected concentration profile was used in CXTFIT2 model (deterministic equilibrium model, MODE CDE) to estimate the dispersion coefficient by an iterative non-linear least square analysis of the data. The mean velocity of the flowing solution, the dispersion coefficient, and the injection

duration for the sample were fitting parameters for this model, while sample initial concentration was assumed known. Afterward, the diffusion coefficient of each sample was calculated using the newly-estimated dispersion coefficient of flow rate and mean velocity in equation (2.13). Details can be viewed in Appendix B.

We also determined the diffusion coefficient by moment analysis of the breakthrough curve (Bello *et al*, 1994). However, our initial work showed that the largest contribution to the experimental error lay in the determination of the second moment. Because of the minor drift of the baseline and the low concentrations on the tails of the BTCs, it is hard to determine the exact second moment, and even minor variations of the second moment would lead to an inaccurate estimation of the diffusion coefficient. Rather than estimate the diffusion coefficients from the various moments, the coefficients were calculated directly by fitting the dispersion equations to the measured absorbency profiles across the eluted solute peaks. This approach was simpler. It was also more accurate because the inevitable propagation of the uncertainties in the moments was eliminated (Leaist, 1991).

3.5 Practical Considerations

The ideal experimental method outlined in Chapter 1 is not practicable for measurements of diffusion coefficients, because it is impossible to construct an apparatus to exactly conform to the ideal. In order to perform such measurements using the same principle, it was therefore necessary to make

changes to the experimental method and to examine the ways in which a practical instrument differs from the ideal. In the following section we examine the consequences of these considerations for the design of an instrument and the working equations for the analysis of experimental parameters.

Reduction of apparatus-induced dispersion and enhancement of diffusion

The dispersion and diffusion mechanisms are always coupled during the process of solute flow and transport. We can see how to reduce apparatus induced dispersion by considering the various terms in equation (2.9). As a general rule, we could not change the diffusion coefficients because they are physical properties of our solutes. However, we could use low velocities, $\overline{V}$, to reduce Taylor dispersion. We could use small bore tubes with small values of R, though this often produces large pressure drops. Even as $\overline{V}$ and R become very small, we will always have some dispersion from axial diffusion, which we neglected.

Helix effects on solute diffusion

Equations (2.6) and (2.7) were derived on the assumption that the tube was straight. This was difficult to realize in practice because of its great length. It was necessary either to bend the tube into a U-shape or to wind it in the form of a helix. When a helical form is used, different positions across the tube, with a slightly different helix radius, experience a slightly different non-ideal velocity, which tends to increase dispersion. In addition, the helical form sets up

secondary flow, which decreases dispersion. These additional effects are a function of w (ratio of the radius of the helix to that of the tube), and the Reynolds (Re), Dean (De) and Schmidt (Sc) numbers which are defined by the following equations (Alizadeh *et al*, 1980)

$$\mathrm{Re} = 2\overline{VR}\rho/\eta \qquad (3.3)$$

$$Sc = \eta/\rho D \qquad (3.4)$$

$$De = \mathrm{Re}\, w^{-1/2} \qquad (3.5)$$

where η represents the shear viscosity and ρ the density of the flowing liquid. In order to minimize curvature effects which create secondary flow, conditions must be chosen so that $De^2 Sc \leq 20$, $\mathrm{Re} < 2000$, and that $w \geq 100$ (Alizadeh *et al*, 1980). With our experimental parameters, $De^2 Sc = 0.022$, and $w = 288$, meeting these conditions. In addition, our low Reynolds number (≈ 0.0088) indicates the laminar flow conditions of our experiment. Any correction for the helical form approaches zero at this very low Reynolds number.

Non-uniform cross-sectional area of tube

The non-uniform cross-sectional area of the tube might affect the concentration distribution of the solute passing through the detector point (Alizadeh, *et al*, 1980), which has not been accounted for in this discussion. We employed the average tube radius determined by the pressure differential method to be the ideal uniform tube radius for calculating the diffusion coefficients.

Finite injection volume

In the theory, the injection pulse is a δ function, which can never be realized in practice. Levenspiel and Smith (1957) have shown that the error arising from this is negligible provided that the volume of the injected sample does not exceed 1 percent of the volumes of the diffusion tube. This holds for our experiment because the injection value was approximately 5 μl, while the volume of diffusion tube was approximately 1022 μl.

Chapter 4

Results and Discussion

4.1 Diffusion Coefficients of KCl, KBr, KI and Benzoic Acid in Type I Water

In order to test the validation of our instrumentation and methods, we measured the diffusion coefficients of KCl, KBr, KI and benzoic acid in Type I water. These model compounds were chosen because their diffusion coefficients (D) are well known (Cussler, 1997, Robinson *et al.,* 1960) and cover a wide range of D values from about 1.0×10^{-9} to 2.02×10^{-9} m^2 s^{-1}. In addition, the fluorobenzoic acids and inorganic anions Br^-, Cl^-, and I^- are also the common tracers used in the hydrologic tracers' test because of their conservative properties and stability in groundwater (Bowman, 1984).

We first carried out experiments to determine a correlation between the output voltage from the UV detector and the initial concentration of each solute. Details can be viewed in Appendix H. For example, Figure 4.1 shows that the output voltage from the UV detector was linearly proportional to the concentration of benzoic acid in water. Such a standard correlation can be made for each solute. We found that there was an almost perfect linear correlation between the voltage reading and the concentration at the range of low concentrations

employed. Thus, the initial concentrations of all solutes were chosen to be 0.1 mM for FBAs and DCBAs in our diffusion coefficient measurements.

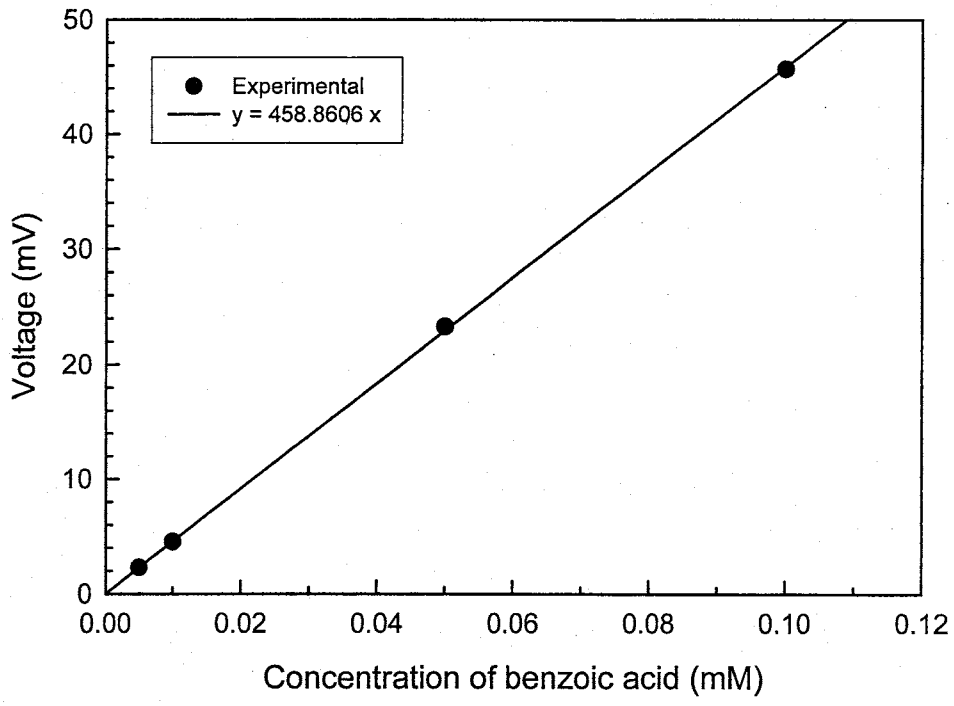

Figure 4.1 Output voltage from UV detector versus the concentration of benzoic acid in water

Figure 4.2 shows the dispersion breakthrough profiles of KCl, KBr, KI and benzoic acid in D.I. water. The dispersion profiles of KCl, KBr, KI and benzoic acid in water were detected at different wavelengths in order to maximize their sensitivity and normalized for the sake of clarity. A flow rate of 0.1 ml/min was used for all model chemicals. The dispersion profile of benzoic acid was much

wider than those of KCl, KBr and KI, indicating that the diffusion coefficient of benzoic acid is much smaller than those of the alkali halides.

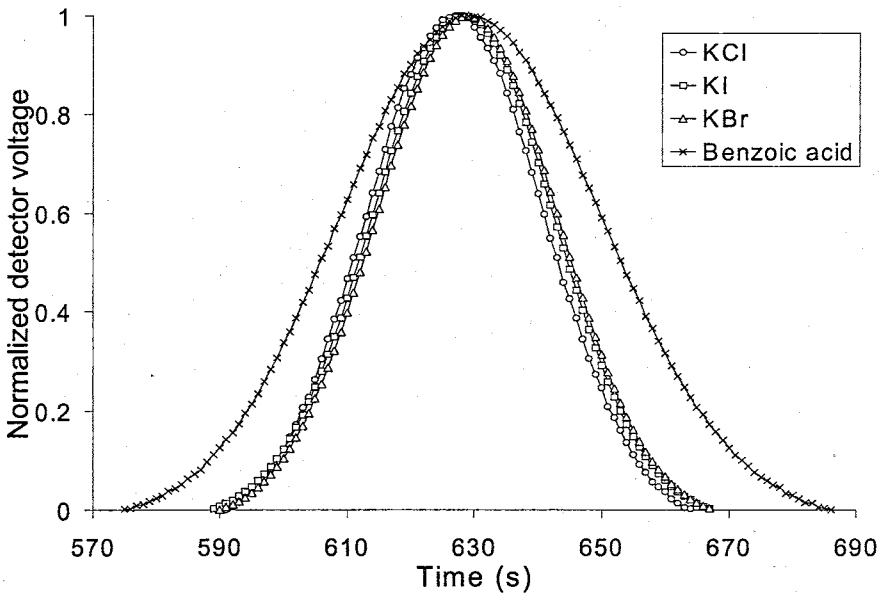

Figure 4.2 The dispersion profiles of KCl, KBr, KI and benzoic acid in water

The measured detector output voltages were converted into the concentration based on the linear correlations as shown in Figure 4.1. The concentration profile for each chemical was fitted using a nonlinear least square procedure in the CXTFIT2 program. As an example, Figure 4.3 shows a typical excellent fit, in this case for benzoic acid in water. The fitted curve is slightly broader at the two tails, which may potentially lead to an underestimation of the diffusion coefficient based on this fitting procedure. The diffusion coefficient was

eventually calculated from the diffusion coefficient based on the nonlinear least-square fit.

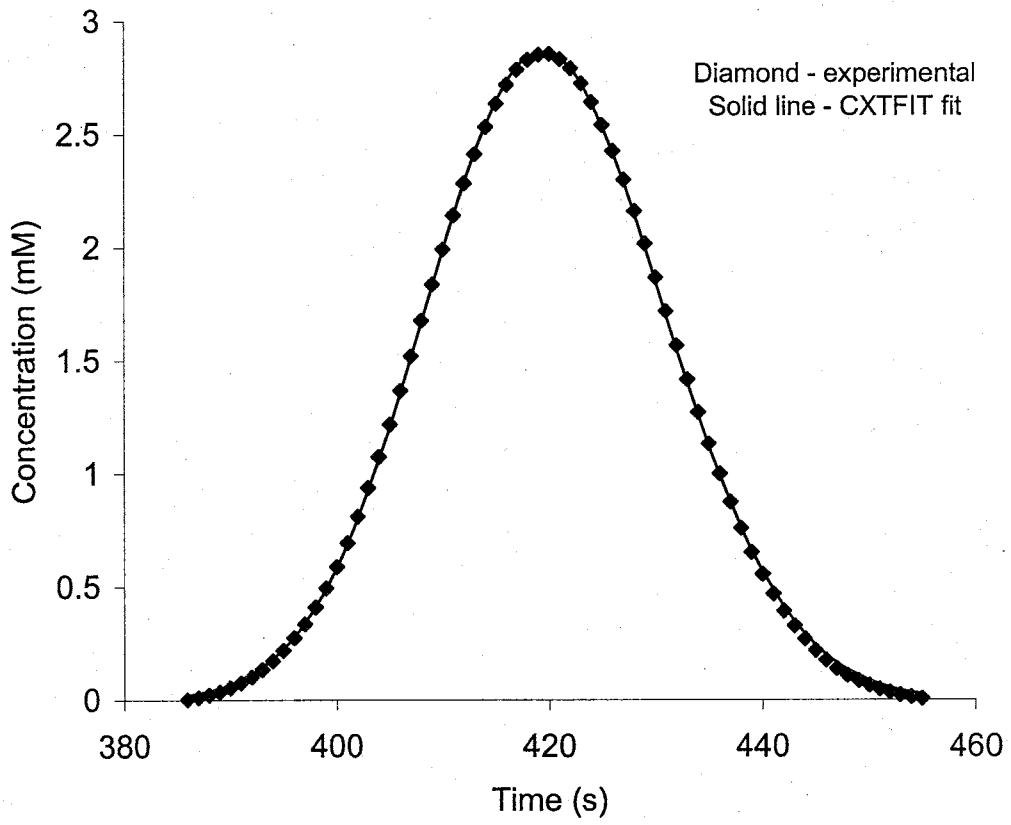

Figure 4.3 Concentration profile of benzoic acid in water

Our experimental diffusion coefficients for KCl, KBr, KI and benzoic acid measured at a constant flow rate of 0.1 ml / min are given in Table 4.1. Published diffusion coefficient values are also given in this table for comparison. We can see that the diffusion coefficients of these compounds comport with published data, within an accuracy of 5 percent, indicating that our instrumental system and

methods can be effectively used to measure the diffusion coefficients of other chemicals.

Table 4.1 Diffusion coefficients of KCl, KI, KBr and benzoic acid in water

Chemicals	Our work					Literature *
	In put Concentration (mM)	Detector wavelength (nm)	Diffusion coefficient ($m^2 s^{-1} \times 10^{-9}$)			Diffusion coefficient ($m^2 s^{-1} \times 10^{-9}$)
			Mean	Standard deviation	No. of measure-ments	
KCl	2	190	2.00	0.06	3	2.00
KBr	2	208	1.97	0.02	2	2.02
KI	2	226	1.91	0.01	3	2.00
Benzoic acid	0.1	190	0.97	0.01	2	1.00

* Diffusion coefficients of KCl, KBr and KI are cited from Robinson *et al.* (1960) based on infinitely dilute solution; and the diffusion coefficient of benzoic acid from Cussler (1997) based on infinitely dilute solution.

The diffusion coefficients of the common inorganic tracer anions such as Br^-, Cl^- and I^- are in the range of 1.9 - 2.0 × 10^{-9} m^2 s^{-1}. Among alkali halides, the diffusion coefficient of KI was slightly smaller than those of KCl and KBr. In contrast, the measured diffusion coefficient for benzoic acid is 0.97 × 10^{-9} m^2 s^{-1}, significantly different from those of alkali halides, due to the different chemical and structural properties. Only at very low pore-water velocities, where molecular

diffusion represents a significant component of hydrodynamic dispersion, would these differences in diffusion coefficients cause variations in the macroscopic transport behavior of the different tracers in soils and groundwater (Bowman & Gibbens, 1992).

We also investigated the effect of the initial concentration on the diffusion coefficient. For example, the diffusion coefficients of KCl at different concentrations in water were measured three times at 25 °C and a flow rate of 0.1 ml/min. The results are given in Table 4.2, in comparison with the diffusion coefficient of KCl from references (Harned *et al.*, 1949, Robinson *et al.,* 1960 and Lobo *et al.*, 1998). It can be seen that the diffusion coefficient of KCl in water decreases slightly with increasing concentrations of KCl, probably due to the increasing viscosity and density of the solution. In addition, the experimental diffusion coefficients of KCl at different concentrations are in good agreement (within 2 percent) with the data determined using different methods in literature, which again demonstrates the validation of our developed instrument and methods.

Table 4.2 Diffusion coefficient of KCl at different concentrations in water

Concentration (mM)	Our work (standard-deviation) ($m^2 s^{-1} \times 10^{-9}$)	Harned *et al.* (1949) ($m^2 s^{-1} \times 10^{-9}$)	Robinson & Stokes (1960) ($m^2 s^{-1} \times 10^{-9}$)	Lobo (1998) ($m^2 s^{-1} \times 10^{-9}$)
	Taylor dispersion method	Diaphragm cell method	Diaphragm cell method	Diaphragm cell method
0	-	2.00	2.00	-
2	2.00 (0.06)	-	-	1.98
5	1.99 (0.00)	-	-	1.96
10	1.93 (0.01)	1.91	-	1.89
20	1.90 (0.00)	-	-	-

4.2 Diffusion Coefficient of Fluorobenzoic Acids (FBAs) and Two Dichlorobenzoic Acids (DCBAs) in Aqueous Solutions

Figure 4.4 shows the framework structure of the benzoic acid group, with the numbers from 1 to 6 marked as the substitution sites. The COO^- group is always fixed at site 1. When two, three, four, and five hydrogen atoms in the benzene ring are substituted with fluorine atoms, the fluorobenzoic acids formed are called difluorobenzoic acids (DFBA), trifluorobenzoic acids (TFBA), tetrafluorobenzoic acids (TeFBA), and pentafluoroebenzoic acid (PFBA), respectively. In addition, when the hydrogen atom at site 2 or 3 is substituted by

the CF_3 group, the benzoic acid formed is called *o*-trifluoromethyl-benzoic acid (TFMBA) or *m*-trifluorobenzoic acid (TFMBA), respectively.

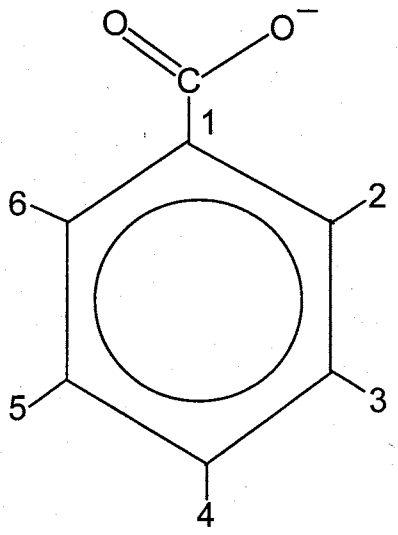

Figure 4.4 The framework structure of benzoic acid and its substitution positions

Benzoic acid, fluorobenzoic acids (FBAs), and dichlorobenzoic acids (DCBAs) have recently been used as water tracers in a variety of hydrologic environments (Bowman & Gibbens, 1992; Meigs *et al.*, 2000). Due to their importance in hydrology of groundwater, we measured the diffusion coefficients of these molecules in Type I water and a buffer solution of 0.1 M potassium

phosphate at 25 °C. In addition, we also measured the diffusion coefficients of two dye tracers (Uranine and Brilliant Blue FCF) in Type I water (Appendix F). Benzoic acid, FBAs and DCBAs are all weak acids, and their dissolution into water results in a mixture of anionic and neutral forms. The ratio of anion to neutral species would increase with the increasing pH. In order to keep all of the acid in the anionic form, and to measure the diffusion coefficient of the anion, not a mean diffusion coefficient for an anion/cation pair (as we did for the alkali halides), we thus measured the diffusion coefficients of these compounds in a buffer solution of 0.1 M potassium phosphate that was adjusted to pH 7.0, as well as in water. The diffusion coefficient measurements were carried out at an injected sample concentration of 0.1 mM, a constant flow rate of 0.1 ml/min, and a fixed detector wavelength of 190 nm. The diffusion coefficient data of all compounds in water and the buffer solution of potassium phosphate were summarized in Table 4.3. In this table, the diffusion coefficient data were averages of at least three well replicated measurements, and the pH of FBAs and CFBAs in Type I water are given in the blackets. In addition, the acid dissociation constant, pK_a, (Benson & Bowman, 1994), molecular weight, and theoretical diffusion coefficients of these chemicals are also given in Table 4.3. Statistical analysis of variance for raw diffusion coefficient data can be viewed in Appendix E.

Table 4.3 Diffusion coefficients of fluorobenzoic acids (FBAs) and dichlorobenzoic acids (DCBA) in water and in buffer solution
(Numbers in parentheses are standard deviations for triplicate measurements)

Chemicals	Diffusion coefficient ($m^2s^{-1} \times 10^{-9}$)				pK_a#	Molecular weight
	Experimental			Calculated* (in water)		
	Water	pH	Buffer			
Benzoic acid	0.97 (0.01)	4.00	0.94 (0.06)	0.85	4.21	122.0
2,3 DFBA	0.98 (0.03)	4.08	0.94 (0.03)	0.81	3.29	158.1
2,4 DFBA	0.93 (0.04)	4.19	0.91 (0.02)	0.81	3.58	158.1
2,5 DFBA	0.95 (0.01)	4.19	0.94 (0.03)	0.81	3.30	158.1
2,6 DFBA	0.88 (0.01)	4.20	0.95 (0.03)	0.81	2.85	158.1
3,4 DFBA	0.95 (0.02)	4.34	0.82 (0.02)	0.81	3.83	158.1
3,5 DFBA	0.92 (0.02)	4.28	0.86 (0.02)	0.81	3.59	158.1
2,3,4 TFBA	0.94 (0.03)	4.24	0.92 (0.00)	0.79	3.30	176.1
2,3,6 TFBA	0.95 (0.02)	4.10	0.83 (0.03)	0.79	2.82	176.1
2,4,5 TFBA	0.94 (0.02)	4.20	0.82 (0.01)	0.79	3.28	176.1
2,4,6 TFBA	0.95 (0.03)	4.15	0.84 (0.03)	0.79	2.83	176.1
3,4,5 TFBA	0.95 (0.02)	4.30	0.87 (0.05)	0.79	3.54	176.1
2,3,4,5 TeFBA	0.95 (0.02)	4.24	0.89 (0.02)	0.78	3.08	194.1
2,3,5,6 TeFBA	0.85 (0.01)	4.20	0.81 (0.04)	0.78	2.71	194.1
PFBA	0.93 (0.01)	4.10	0.74 (0.01)	0.76	2.72	212.1
m-TFMBA	0.88 (0.01)	4.44	0.79 (0.06)	0.74+	3.8	188.1
o-TFMBA	0.86 (0.01)	4.30	0.81 (0.06)	0.73	3.0	188.1
2,4 DCBA	0.89 (0.03)	4.25	0.82 (0.05)	0.71		191.0
3,5 DCBA	0.87 (0.01)	4.35	0.87 (0.05)	0.71		191.0

* Estimated by the Hayduk and Laudie method (1974)
\+ Measured value (Bowman, 1984b))
\# Benson and Bowman (1994)

Table 4.3 shows that the measured diffusion coefficient in the buffer solution of 0.1 M potassium phosphate was normally lower than that in water. There were two possible causes for this observation: first, the diffusion medium of potassium phosphate buffer solution becomes more viscous than pure water; ionic strength are also different within these two medium; second, the pH condition of the solution may affect the diffusion of the solutes.

The calculated theoretical diffusion coefficients of these compounds in water are consistently 10% smaller than those measured in water (Figure 4.5). In the calculation method used in this work, only the numbers of fluorine atoms around the benzene ring were considered. However, the non-symmetry of different fluorobenzoic acid molecules may dramatically affect their diffusion coefficient. For example, 2,6 DFBA should be strongly hydrated only towards the carboxyl end of the molecule, while 3,5 DFBA should be more uniformly hydrated. The hydration differences for these two molecules would be likely affect their diffusion coefficients. However, these important factors are not considered in our calculation of diffusion coefficients, and thus we may need to develop new model that include such factors as molecular configuration and orientation relaxation, as well as molecular weight, in the calculation of diffusion coefficients.

In order to more clearly demonstrate the relationship of the diffusion coefficient with molecular weight, we plotted the diffusion coefficients of the FBAs and CBAs in water and 0.1 M potassium phosphate buffer against their molecular weights (Figure 4.6). We found that the measured diffusion coefficients

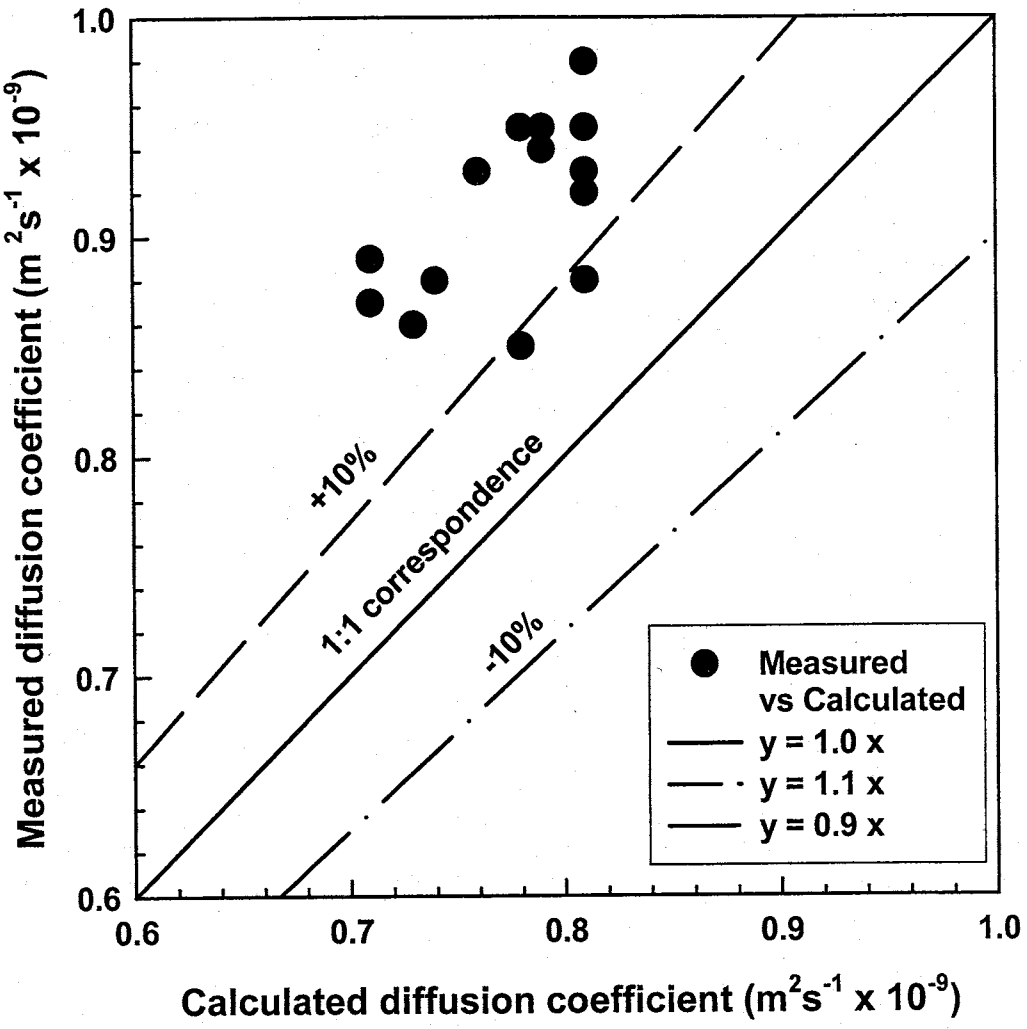

Figure 4.5 Measured diffusion coefficients versus calculated diffusion coefficients of FBAs in water

of these compounds either in water or in 0.1 M potassium phosphate buffer solution showed a general trend of decreasing diffusion coefficient with increasing molecular weight. This correlation was quite poor for the case of the diffusion coefficient of these compounds in water (Figure 4.6 a). For example, the diffusion coefficients of fluorobenzoic acids (*e.g.*, DFBA and TeFBA) of the same molecular weight varied markedly. However, this correlation was much better for the case of diffusion coefficients of these compounds in potassium phosphate buffers of pH 7.0 (Figure 4.6b), although the diffusion coefficients of the fluorobenzoic acids (*e.g.*, DFBA, TFBA and TeFBA) of the same molecular weight still varied. However, the analysis in Appendix E shows that in a buffer solution there was no statistically significant difference in the mean diffusion coefficients of most FBAs with the same molecular weight, which was contrary to the case measured in water. These results suggest that the diffusion coefficient of these molecules in aqueous solutions intrinsically depends not only on molecular weight, but also on their geometrical configurations and pH of solutions. Thus, estimating the diffusion coefficients of these chemicals in water simply based on their molecular weight alone can result in a significant error.

Similarly, we plotted the diffusion coefficients against the acid dissociation constant (pK_a) of FBAs in water and the buffer solution (Figure 4.7), according to the data given in Table 4.3. The correlation between diffusion coefficients of FBAs in water and their acid dissociation constant was poor. All of these results indicate that the chemical diffusion of molecules in aqueous solution is a very complicated process, depending not only on the intrinsic factors of molecules

(*e.g.*, molecular weight, geometrical configuration and dissociation constant), but also on external factors (*e.g.*, pH of solution, viscosity, and concentration).

Like most weak electrolyte solutions, FBAs diffuse in solution as molecular species together with ions produced by dissociation. The various solute species react rapidly enough to maintain chemical equilibrium at each point along the diffusion path. Thus, diffusion in a binary solution of FBAs is described by a single diffusion coefficient regardless of the number of different solute species present. On the other hand, the dissociation of FBAs influences the rate of their diffusion in two important ways: first, it increases the chemical potential gradient that drives the FBAs through water; second, because movement of two separate ions experiences more frictional resistance than transport of a single molecular species, dissociation tends to reduce the mobility of FBAs (Leaist, 1991). The interpretation of the diffusion coefficients in water is complicated by the fact that different FBAs have different ratios of neutral to anionic form. However, at the low concentrations ($\leq$ 0.1mM) in the diffusion coefficient measurements both in water and a buffer solution, we can neglect the complications arising from viscosity changes of the solution, counterflow of solvent, and dimerization of acids. Electrophoretic corrections also are very small for this system. Thus, because the measurement was made at a low concentration, we believe that the results (determined both in water and a buffer solution) we reported here are reliable parameters needed to evaluate transport processes.

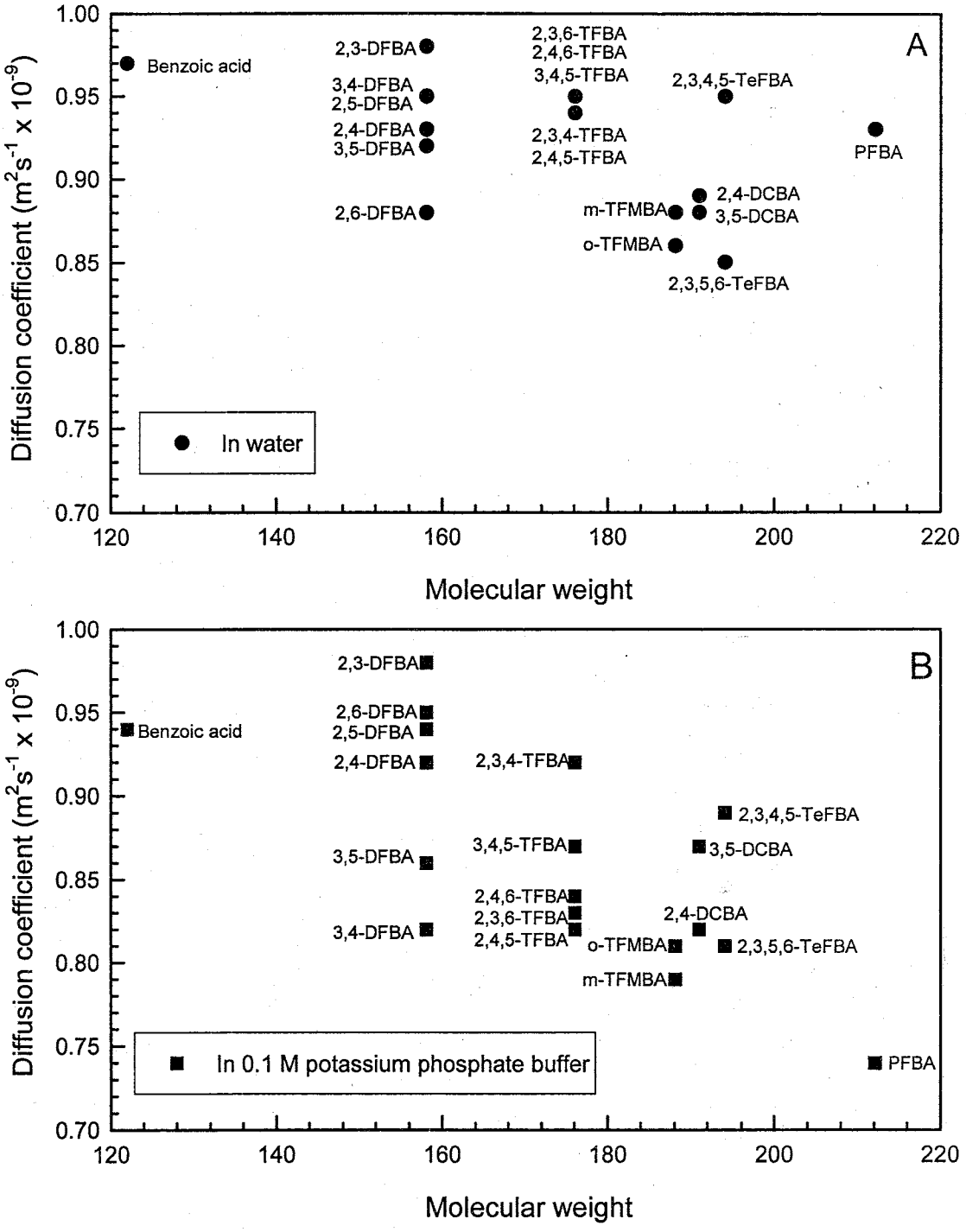

Figure 4.6 Diffusion coefficients of FBAs in water (A) and 0.1 M potassium phosphate buffer (B) versus molecular weights

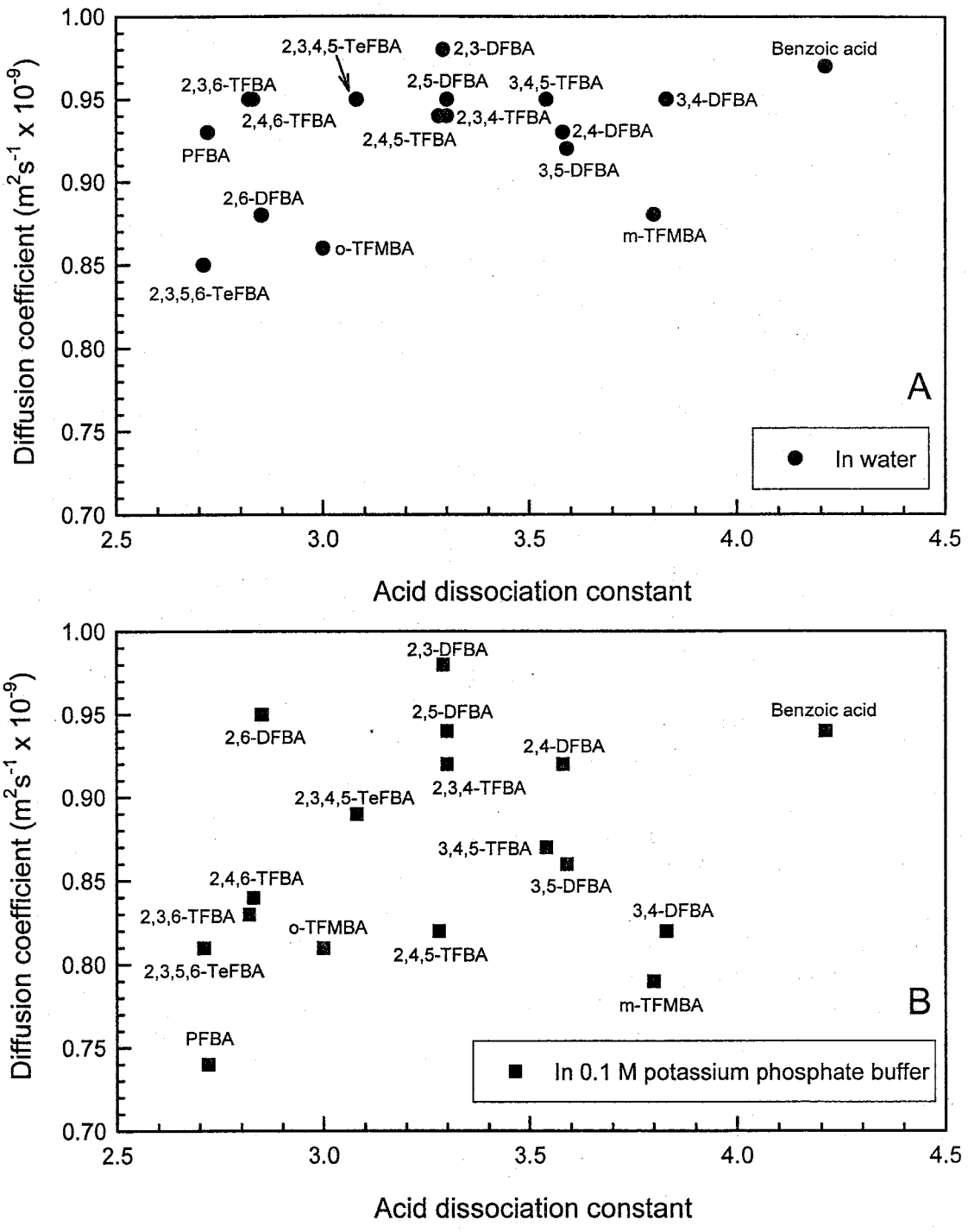

Figure 4.7 Diffusion coefficients of FBAs in water (A) and 0.1 M potassium phosphate buffer solution (B) versus pK_a

Chapter 5

Summary and Future Work

5.1 Summary

Water tracers are used to characterize hydrological processes (*e.g.*, water flow direction and velocity, water flux, solute dispersion, sorption and retardation) in rivers, lakes, soils and aquifers. Inorganic anions such as Cl^-, Br^- and I^-, and benzoic acid derivatives such as flurobenzoic acids (FBAs) have proven to be good hydrological tracers (Bowman & Gibbens, 1992). Diffusion coefficients of these hydrological tracers and other solutes in aqueous solutions are important parameters for hydrological modeling. Although the diffusion coefficients of alkali halides have been measured experimentally, and those of some FBAs and CBAs have been estimated using the Hayduk & Laudie method (Benson & Bowman, 1994), the experimental diffusion coefficient data of FBAs and CBAs are largely lacking in published studies.

We developed an experimental system for measuring the diffusion coefficients of hydrologic tracers and other trace solutes in aqueous solutions according to the Taylor dispersion technique. We completed experimental design and testing both for continuous and discrete sampling. The discrete sampling

was required for high ionic strength solutions (details can be viewed in Appendix C). After a certain amount of solute was injected into the sample column using a syringe, a dispersion profile of absorbance voltage recorded by a UV detector was measured against time.

The recorded voltage was proportional to the concentration, so that the concentration profile over time was obtained. The concentration profiles were fitted using a non-linear, least-square procedure in the CXTFIT2 program (Toride *et al.*, 1995) to calculate the diffusion coefficients.

We thus measured the diffusion coefficients of KCl, KBr, KI and benzoic acid in Type I water and found that our results corroborated those of published data within an accuracy of 5 percent. We also found that the diffusion coefficient of KCl in water decreased slightly with increasing initial concentrations, and our measured diffusion coefficient of KCl at different concentrations were within 2 percent of published data. Therefore, our developed experimental system and methods can be effectively used to measure diffusion coefficients of trace solutes of important interests in chemistry and hydrology.

We also measured the diffusion coefficients of a suite of fluorobenzoic acids (FBAs) and two chlorobenzoic acids (DCBAs) in Type I water and 0.1 M potassium phosphate buffer solution. The diffusion coefficients of FBAs and DCBAs in D.I. water were consistently greater than those calculated from molecular structure. Also, the diffusion coefficients of these chemicals in D.I. water, in which pH was reduced to 4.00-4.44 due to the dissociation of these

weak acid chemicals, were consistently greater than those in potassium phosphate buffer solutions in which pH was adjusted to 7.0. The correlations of diffusion coefficients of FBAs and DCBAs in D.I. water with either the molecular weight or acid dissociation constant were quite poor. However, in 0.1 M potassium phosphate buffer solution, the diffusion coefficient for FBAs tended to decrease with increasing molecular weight , although these correlations are quite scattered. In addition, for each FBAs group (*e.g*, DFBA, TFBA, or TeFBA) of the same molecular weight, the diffusion coefficients calculated theoretically are the same for each member of the same group, because the calculated diffusion coefficients are estimated according to aqueous diffusion of a spherical molecule in water (Tucker & Nelken, 1982). However, our measured diffusion coefficients among the different isomers of the same FBA group varied markedly and also were different from the calculated data, probably due to the geometrical configuration of the molecules. Thus, the diffusion coefficients of FBAs and DCBAs are related to both the intrinsic properties of molecules (*e.g.*, molecular weight, geometrical configuration) and external factors (*e.g.*, temperature, pH, density, and viscosity of medium solution).

5.2 Future Work

Our developed instrument and methods for measuring diffusion coefficients of hydrological tracers and other solutes in aqueous solutions would have tremendous applications in hydrology, environmental engineering and chemical engineering. However, there is also opportunity for experimental

improvements and tremendous potential for using this technique for extended applications in the future.

For example, we are able to introduce an advanced electronic system for automated sample injection, so that we can run about 100-200 Taylor experiments per week, greatly improving the efficiency of data collection relative to traditional diffusion experiments using an interferometer or a diaphragm cell, and also minimizing the effect of a possible dispersion on the solute diffusion process. An electronic actuator can be used with the injector. Up to this point we have injected samples manually by turning a knob. The new actuator, controlled by our system computer, will provide more precise injections along with a more accurate measurement of the injection start time. We can utilize a more accurate pump system to ensure the steady flow of solution, and improve our experimental system to eliminate the effects of external factors (*e.g.*, temperature gradient) on the diffusion process. In addition, because widths and asymmetries are normally measured using chromatographic data systems, we need to develop a more effective software system for data collection in order to improve the accuracy of the monitored dispersion profile. The input file used in CXTFIT2 program for data analysis should be re-evaluated since activity coefficient instead of concentration of solute should be used to calculate the diffusion coefficient.

Theoretically, the measurement of diffusion coefficients should not change with flow rates of the mobile phase, and previous studies seldom mentioned the flow rate effects on the measurement of the diffusion coefficient. However, we

observed that the diffusion coefficient measured in our experiments changed with the flow rates and we can not explain why (Appendix D).

We could extend both the Taylor dispersion technique and our developed experimental system to measure the diffusion coefficients of either conservative or reactive solutes in high concentrations, and to measure the diffusion coefficient in multiple-component systems. In aqueous solutions that contain more than one solute, the diffusive transport of one solute may be affected by the concentration gradients; or, more strictly, the activity gradients of the other solutes. Thus, to study diffusion coefficients of aqueous solution systems of high concentrations and/or multiple-components are challenging experimentally, but very important in the fields of hydrology, environmental science, biology, chemistry, and chemical engineering.

References

Aris, R., On the dispersion of a solute in a fluid flowing through a tube, *Proc. Royal Soc. Lond.*, **A235**, 67, 1956.

Alizadeh, A, C., Nieto de Castro, C. A., and Wakeham, W. A., The theory of the Taylor dispersion technique for liquid diffusivity measurements, *Int. J. Thermophys.*, **1**(3), 243-284, 1980.

Bello, M. S., Rezzonico, R., and Righetti, P. G., Use of Taylor - Aris dispersion for measurement of a solute diffusion coefficient in thin capillaries, *Science,* **266**, 773-776, 1994.

Benson, C. F., and Bowman, R. S., Tri- and tetrafluorobenzoates as nonreactive tracers in soil and groundwater, *Soil Sci. Soc. Am. J.*, **58**, 1123-1129, 1994.

Bish, D. L., and Aronson, J. L., Paleogeothermal and paleohydrologic conditions in silicic tuff from Yucca Mountain, Nevada, *Clays and Clay Minerals*, **41**, 148-161, 1993.

Bolivar, S., Broxton, D. E., Bish, D. L., Byers, F., Carlos, B. A., Levy, S. S., Vaniman, D. T., and Chipera, S. J., Mineralogy-petrology studies and natural Barriers at Yucca. Mountain, Nevada, In "*Proceedings of the Topical Meeting on Nuclear Waste Isolation in the Unsaturated Zone* (FOCUS '89)", 125-133, 1990.

Bowman, R. S., Analysis of soil extracts for inorganic and organic tracer anions via high-performance liquid chromatography, *Journal of Chromatography*, 285, 467-477, 1984a.

Bowman, R. S., Evaluation of some new tracers for soil water studies. *Soil Sci. Soc. Am. J.*, **48**, 987-993, 1984b.

Bowman, R. S., and Gibbens, J. F., Difluorobenzoates as nonreactive tracers in soil and groundwater, *Groundwater*, **30**(1), 8-13, 1992.

Cohen, R. M., and Mercer, J. W., DNAPL Site_Evaluation, Smoley, Boca Raton, Florida, 1993.

Cussler, E. L., *Diffusion Mass Transfer in Fluid Systems* (2nd edition), Cambridge University press, 1997.

Duda, J. L., Vrentas, J. S., Ju, S. T., and Liu, H. T., Predication of diffusion coefficients for polymer-solvent systems, *AIChE J.*, **28**, 279, 1982.

Espinosa, P. J., and Garcia de la Torre, L., Theoretical predication of translational diffusion coefficients of small rigid molecules from their molecular geometry, *J. Phys. Chem.*, **91**, 3612, 1987.

Fetter, C. W., *Contaminant Hydrology* (2nd edition), Prentice Hall, New Jersey, 1999.

Hao, L., "*Multicomponent interdiffusion in micellar solutions and microemulsions*", Ph. D. Thesis, The University of Western Ontario, Canada, 1996.

Harned, H. S., and Nuttall, R. L., The diffusion coefficient of potassium chloride in dilute aqueous solution at 25 °C, *J. Am. Chem. Soc,* **71**, 1460, 1949.

Hayduk, K. W., and Laudie, H., Prediction of diffusion coefficients for non-electrolysis in dilute aqueous solutions, *AIChE J.*, **20**, 611-615, 1974.

Leaist, D. G., Ternary diffusion coefficients of 18 - Crown - 6Ether – KCl water by direct least squares analysis of Taylor dispersion measurements, *J. Chem. Soc. Farady Trans.,* **87** (4), 597-601, 1991.

Leaist, D. G., Determination of ternary diffusion coefficients by the Taylor dispersion method, *J. Phys. Chem.*, **94**, 5180-5183, 1990.

Levenspiel, O., and Smith, W. K., Notes on the diffusion-type model for the longitudinal mixing of fluids in flow, *Chem. Eng. Sci.*, **6**, 227, 1957.

Levy, S. S., Mineralogical alteration history and paleohydrology at Yucca Mountain, Nevada, In "*High Level Radioactive Waste Management: proceedings of the Second Annual International Conference*", 477-485, 1991.

Lide , D. R. (*Ed.*), *CRC Handbook of Chemistry & Physics* (73rd Edition), CRC Press, Boca Raton, Florida, 1992.

Lobo, V. M. M., Ribeiro, A. C. F., and Verissimo, L. M. P., Diffusion coefficients in aqueous solutions of potassium chloride at high and low concentrations, *J. Mol. Liquids*, **78**, 139-149, 1998.

Loh, W., Taylor dispersion technique for investigation of diffusion in Liquids and its applications, *QUIMICA NOVA*, **20**, 541-545, 1997.

Lyman, W. J., Reehl, W. F. and Rosenblatt, D. H., *Handbook of Chemical Property Estimation Methods*, McGraw-Hill, New York, 1984.

Meigs, L. C., Beauheim, R. L. and Jones, T. L., 2000, Interpretations of Tracer Tests Performed in the Culebra Dolomite at the Waste Isolation Pilot Plant Site, SAND 97-3109, Sadia National Laboratory.

Noulty, R. A., and Leaist, D. G., Diffusion coefficient of aqueous benzoic acid at 25 °C, *J. Chem. Eng. Data*, **32**, 418-420, 1987.

Othmer , D.F., and Thakar, M. S., Correlating diffusion coefficients in liquids, *Ind. Eng. Chem.,* **45**, 589-593, 1953.

Reimus, P.W., *Predictions of Tracer Transport in Interwell Tracer Tests at the C-Hole Complex* (Yucca Mountain Site Characterization Project Report Milestone 4077), Los Alamos, NM: Los Alamos National Laboratory, 1996.

Robinson, R. G., and Stokes, R. H., *Electrolyte Solutions*, Butterworths, London, 1960.

Schramke, J. A., and Murphy, S. F., Prediction of aqueous diffusion coefficients for organic compounds at 25 °C, *Chemosphere*, **38**(10), 2381-2406, 1999.

Taylor, G. I., Dispersion of soluble matter in solvent flowing slowly through a tube, *Proc. Royal Soc. Lond.,* **A219**, 186, 1953.

Taylor, G. I., Conditions under which dispersion of a solute in a stream of solvent can be used to measure molecular diffusion, *Proc. Royal. Soc. Lond.,* **A225**, 473, 1954.

Toride, N., Leij, F.J., and Van Genuchten, M.T., *The CXTFIT Code for Esstimating Transport Parameters from Laboratory or Field Tracer Experiments*, U.S. Salinity Laboratory, 1995.

Tyrrell, H. J. V., and Harris, K. R., *Diffusion in Liquids*, Butterworths, London, 1984.

Wilke, C. R., and Chang, P., Correlation of diffusion coefficients in dilute solutions, *Inst. Chem. Eng. J.,* 1, 264-270, 1955.

Wilson, J. L., and Bowman, R. S., Aqueous Diffusion Coefficients for Chemicals of Environmental and Hydrological Interest, *Grant Proposal*, New Mexico Institute of Mining and Technology, 1997.

Wisnudel, M. B., and Torkelson, J. M., Use of Taylor dispersion for the measurement of probe diffusion in polymer solutions, *AIChE. J.*, **42**(4), 1, 1996

Wunderly, M. D., Blowes, D. W., Frind, E. O., and Ptacek, C. J., Sulfide mineral oxidation and subsequent reactive transport of oxidation products in mine tailings impoundments: a numerical model, *Water Resour. Res.*, **32**(10), 3173-3187, 1996.

Yang, X. N., and Matthews. M. A., Diffusion coefficients of three organic solutes in aqueous sodium dodecyl sulfate solution, *J Colloid Interface Sci.*, **229**, 53-61, 2000.

Zhang, S. F., Splendiani, A., Freitas dos Santos, L. M., and Livingston, A. G., Determination of pollutant diffusion coefficients in naturally formed biofilms using a single tube extractive membrane bioreactor, *Biotech. Bioeng.*, **59**(1), 80-89, 1998.

APPENDIX A

Raw Experimental Data

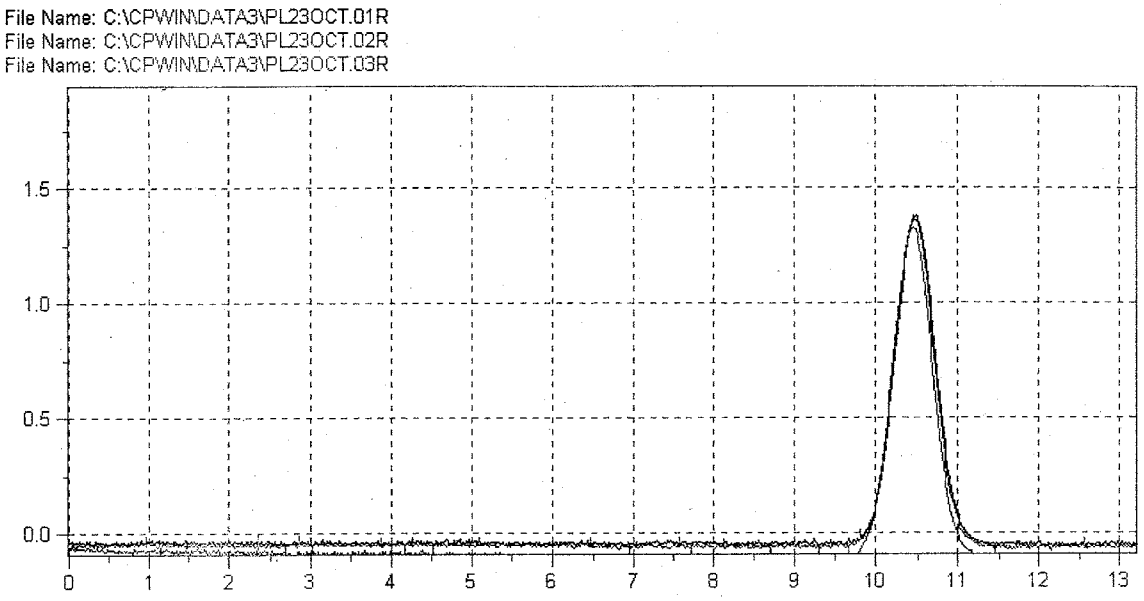

Figure A-1 Three repeatable dispersion profiles of KCl (2 mM) in water at targeted 0.1ml/min

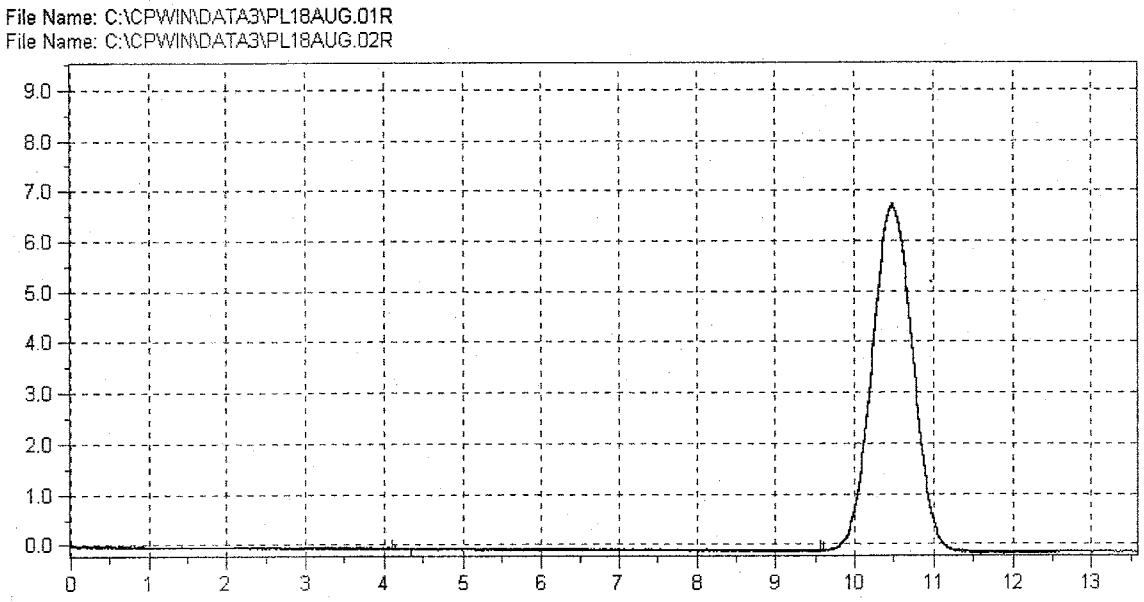

Figure A-2 Two repeatable dispersion profiles of KBr (2 mM) in water at targeted 0.1ml/min

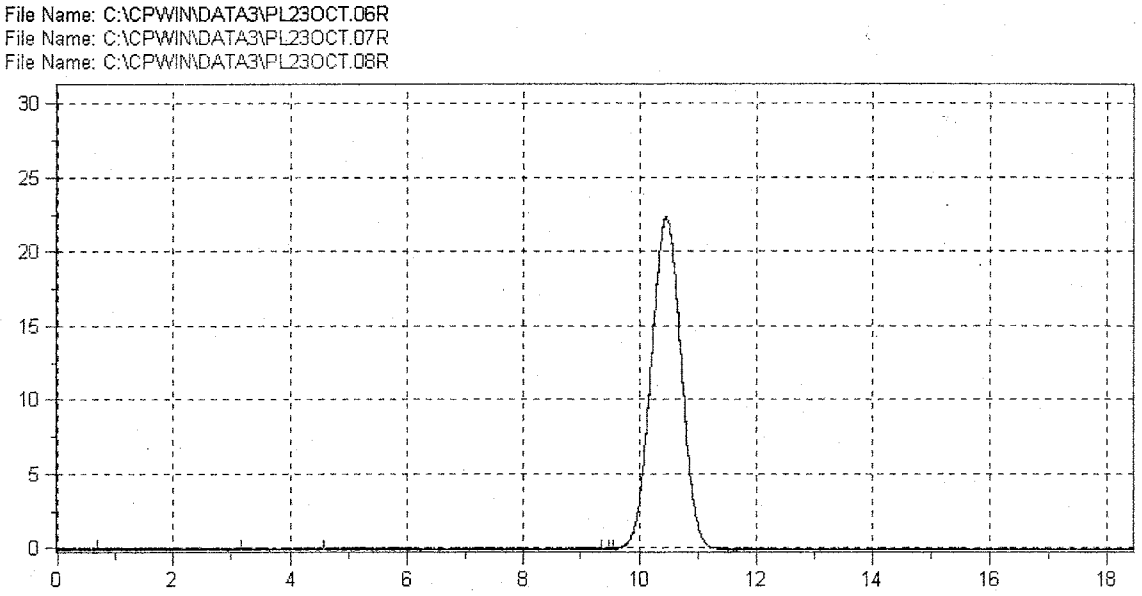

Figure A-3 **Three repeatable dispersion profiles of KI (2 mM) in water at targeted 0.1ml/min**

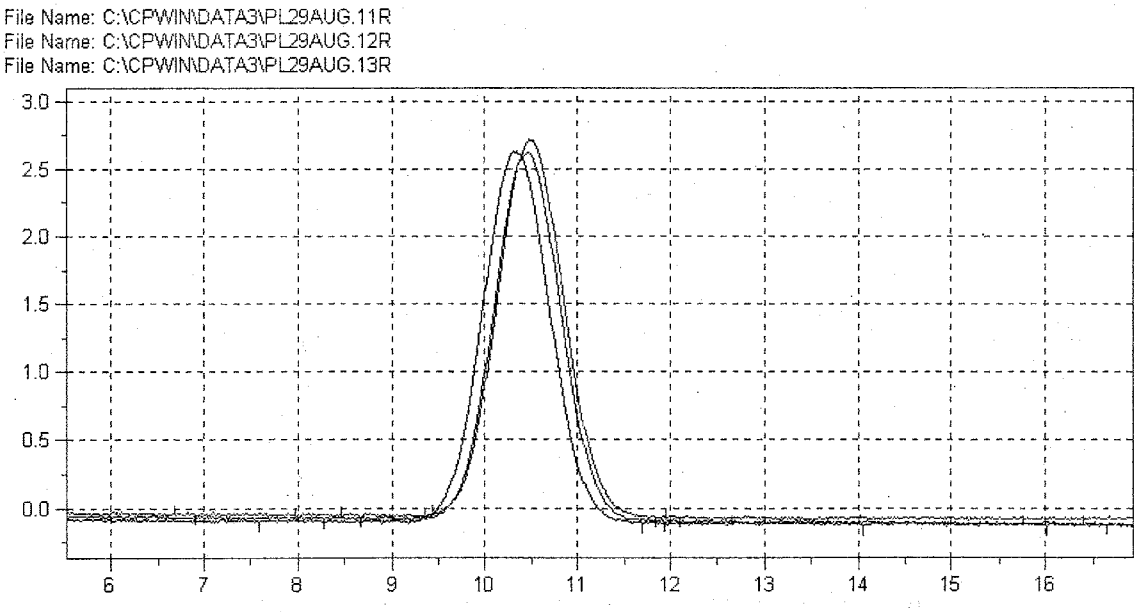

Figure A-4 **Three repeatable dispersion profiles of benzoic acid (0.1mM) in water at targeted 0.1ml/min**

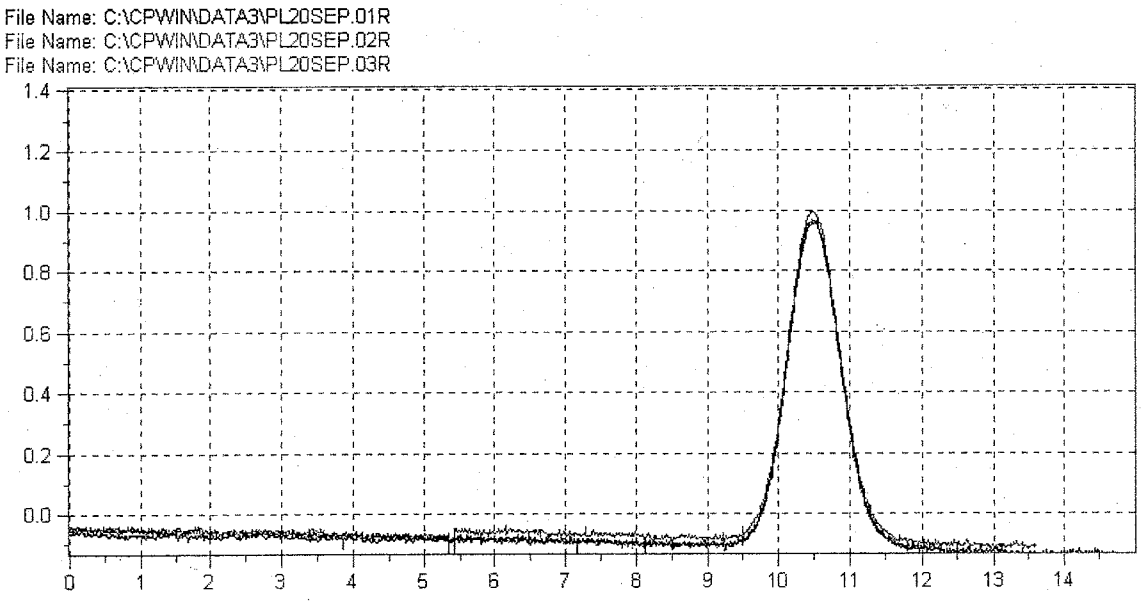

Figure A-5 **Three repeatable dispersion profiles of PFBA (0.1mM) in water at targeted 0.1ml/min**

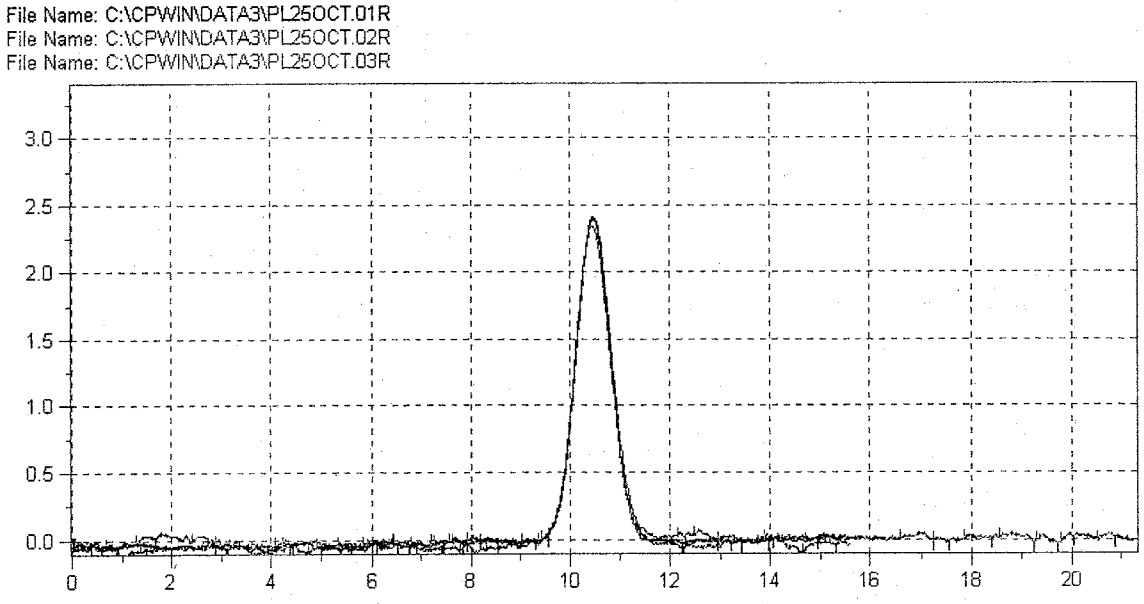

Figure A-6 **Three repeatable dispersion profiles of 2,5 DFBA (0.1mM) in potassium phosphate buffer at targeted 0.1ml/min**

APPENDIX B

Typical CXTFIT2 Model Input / Output Files

B-1 Input files

```
1
*** BLOCK A: MODEL DESCRIPTION
*****************************************
Estimate D for 0.1 mM PFBA in water
Raw experimental file name: pl20sep2
Ping Hu
INVERSE    MODE      NREDU
   1         1         1
 MODC       ZL(BLANK IF MODE=NREDU=1)
   1
*** BLOCK B: INVERSE PROBLEM
*********************************************
  MIT       ILMT    MASS
 150        1       1
*** BLOCK C: TRANSPORT PARAMETERS
***************************************
    V         D         R      Mu
  3.652      3.2       1.0      0.0
  1         1          0        0
1     0.1     999      999
6    10       999      999
*** BLOCK D: BVP; MODB=0 ZERO; =1 Dirac; =2 STEP; =3 A PULSE
************
  MODB                =4 MULTIPLE; =5 EXPONENTIAL; =6 ARBITRARY
 3
0.1   3.21
   0       1
   999    0.1
   999   100
*** BLOCK E: IVP; MODI=0 ZERO; =1 CONSTANT; =2 STEPWISE; =3 EXPONENTIAL
**
  MODI
    0
*** BLOCK F: PVP; MODP=0 ZERO; =1 CONSTANT; =2 STEPWISE; =3 EXPONENTIAL
**
   MODP
    0
*** BLOCK G: DATA FOR INVERSE PROBLEM
************************************
INPUTM =0,Z,T,C :=1,T,C FOR SAME Z ;=2,Z,C FOR SAME T ;=3, ver.1 format
   3
     C         X         T (3F10.0)  (Give "0 0 0" after last data
set.)
0.0000659      2185       584
0.0001517      2185       585
0.0001697      2185       586
0.0002476      2185       587
0.0003068      2185       588
0.0004642      2185       589
0.0004822      2185       590
0.0005968      2185       591
0.0007099      2185       592
0.0007946      2185       593
0.0009280      2185       594
```

0.0010542	2185	595
0.0012033	2185	596
0.0012783	2185	597
0.0014371	2185	598
0.0014940	2185	599
0.0017042	2185	600
0.0018687	2185	601
0.0020140	2185	602
0.0021965	2185	603
0.0024070	2185	604
0.0024887	2185	605
0.0027101	2185	606
0.0028641	2185	607
0.0030960	2185	608
0.0032769	2185	609
0.0034564	2185	610
0.0036224	2185	611
0.0037711	2185	612
0.0038692	2185	613
0.0040659	2185	614
0.0042431	2185	615
0.0043630	2185	616
0.0045878	2185	617
0.0047073	2185	618
0.0048455	2185	619
0.0049999	2185	620
0.0050801	2185	621
0.0051718	2185	622
0.0052569	2185	623
0.0053120	2185	624
0.0054214	2185	625
0.0054150	2185	626
0.0055210	2185	627
0.0055180	2185	628
0.0055360	2185	629
0.0055008	2185	630
0.0054768	2185	631
0.0054423	2185	632
0.0053985	2185	633
0.0053131	2185	634
0.0053236	2185	635
0.0052812	2185	636
0.0051231	2185	637
0.0050505	2185	638
0.0049366	2185	639
0.0048609	2185	640
0.0045848	2185	641
0.0045563	2185	642
0.0043461	2185	643
0.0042506	2185	644
0.0040082	2185	645
0.0038190	2185	646
0.0036995	2185	647
0.0035268	2185	648
0.0033964	2185	649
0.0032118	2185	650
0.0030432	2185	651

0.0029177	2185	652
0.0027603	2185	653
0.0026108	2185	654
0.0023853	2185	655
0.0022602	2185	656
0.0020695	2185	657
0.0019687	2185	658
0.0017941	2185	659
0.0016896	2185	660
0.0015263	2185	661
0.0014206	2185	662
0.0013120	2185	663
0.0011262	2185	664
0.0010816	2185	665
0.0009291	2185	666
0.0008774	2185	667
0.0007407	2185	668
0.0006455	2185	669
0.0005916	2185	670
0.0004424	2185	671
0.0004312	2185	672
0.0002892	2185	673
0.0002754	2185	674
0.0002405	2185	675
0.0001169	2185	676
0.0001491	2185	677
0.0000322	2185	678
0	0	0

B-2 Output files

```
*********************************************************************
      CXTFIT VERSION 2.0 (1/2/95)
      ANALYTICAL SOLUTIONS FOR ONE-DIMENSIONAL CDE
      NON-LINEAR LEAST-SQUARES ANALYSIS
      Estimate D for 0.1 mM PFBA
      Ping Hu
      DATA INPUT FILE:  pl20sep2.in
*********************************************************************


     MODEL DESCRIPTION
     =================
        DETERMINISTIC EQUILIBRIUM CDE (MODE=1)
        FLUX-AVERAGED CONCENTRATION
        REAL TIME (t), POSITION(x)
          (D,V,mu, AND gamma ARE ALSO DIMENSIONAL)


     INITIAL VALUES OF COEFFICIENTS
     ==============================
     NAME         INITIAL VALUE  FITTING   MIN VALUE      MAX VALUE
      V........      .3652E+01      Y      .1000E+01      .6000E+01
      D........      .3200E+01      Y      .1000E+00      .1000E+02
      R........      .1000E+01      N
      mu.......      .0000E+00      N
      Cin......      .1000E+00      N
      T2.......      .3210E+01      Y      .1000E+00      .1000E+03


     BOUNDARY, INITIAL, AND PRODUCTION CONDITIONS
     ============================================
       <INITIAL ESTIMATE OF B.C.>
       SINGLE PULSE OF CONC. =      .1000 & DURATION =     3.2100
       SOLUTE FREE INITIAL CONDITION
       NO PRODUCTION TERM


     PARAMETER ESTIMATION MODE
     =========================
       MAXIMUM NUMBER OF ITERATIONS =  150
       DURATION TIME, T2, IS FITTED TO THE DATA
            .1000 < T2 <  100.0000


     ITER      SSQ         V....      D....      T2...
      0     .1288E-02   .365E+01   .320E+01   .321E+01
      1     .3593E-03   .360E+01   .888E+01   .285E+01
      2     .3089E-03   .338E+01   .867E+01   .214E+01
      3     .5715E-04   .348E+01   .449E+01   .224E+01
      4     .3255E-05   .347E+01   .316E+01   .266E+01
      5     .7818E-06   .348E+01   .352E+01   .269E+01
      6     .7577E-06   .348E+01   .355E+01   .269E+01
      7     .7577E-06   .348E+01   .355E+01   .269E+01
```

COVARIANCE MATRIX FOR FITTED PARAMETERS

	V....	D....	T2...
V....	1.000		
D....	-.171	1.000	
T2...	.007	.580	1.000

RSQUARE FOR REGRESSION OF OBSERVED VS PREDICTED = .99771296
(COEFFICIENT OF DETERMINATION)

NON-LINEAR LEAST SQUARES ANALYSIS, FINAL RESULTS

NAME	VALUE	S.E.COEFF.	T-VALUE	95% CONFIDENCE LIMITS LOWER	UPPER
V....	.3476E+01	.9292E-04	.3740E+05	.3475E+01	.3476E+01
D....	.3554E+01	.1141E-03	.3114E+05	.3553E+01	.3554E+01
T2...	.2691E+01	.1124E-03	.2394E+05	.2691E+01	.2692E+01

----------ORDERED BY COMPUTER INPUT----------

$	NO	DISTANCE	TIME	CONCENTRATION OBS	FITTED	RESI-DUAL
	1	2185.0000	584.0000	.0001	.0003	-.0002
	2	2185.0000	585.0000	.0002	.0003	-.0002
	3	2185.0000	586.0000	.0002	.0004	-.0002
	4	2185.0000	587.0000	.0002	.0004	-.0002
	5	2185.0000	588.0000	.0003	.0005	-.0002
	6	2185.0000	589.0000	.0005	.0005	-.0001
	7	2185.0000	590.0000	.0005	.0006	-.0001
	8	2185.0000	591.0000	.0006	.0007	-.0001
	9	2185.0000	592.0000	.0007	.0008	-.0001
	10	2185.0000	593.0000	.0008	.0009	-.0001
	11	2185.0000	594.0000	.0009	.0010	.0000
	12	2185.0000	595.0000	.0011	.0011	.0000
	13	2185.0000	596.0000	.0012	.0012	.0000
	14	2185.0000	597.0000	.0013	.0013	.0000
	15	2185.0000	598.0000	.0014	.0014	.0000
	16	2185.0000	599.0000	.0015	.0015	.0000
	17	2185.0000	600.0000	.0017	.0017	.0000
	18	2185.0000	601.0000	.0019	.0018	.0001
	19	2185.0000	602.0000	.0020	.0020	.0000
	20	2185.0000	603.0000	.0022	.0021	.0001
	21	2185.0000	604.0000	.0024	.0023	.0001
	22	2185.0000	605.0000	.0025	.0025	.0000
	23	2185.0000	606.0000	.0027	.0026	.0001
	24	2185.0000	607.0000	.0029	.0028	.0001
	25	2185.0000	608.0000	.0031	.0030	.0001
	26	2185.0000	609.0000	.0033	.0032	.0001
	27	2185.0000	610.0000	.0035	.0033	.0001
	28	2185.0000	611.0000	.0036	.0035	.0001
	29	2185.0000	612.0000	.0038	.0037	.0001
	30	2185.0000	613.0000	.0039	.0039	.0000
	31	2185.0000	614.0000	.0041	.0041	.0000
	32	2185.0000	615.0000	.0042	.0042	.0000

33	2185.0000	616.0000	.0044	.0044	.0000
34	2185.0000	617.0000	.0046	.0046	.0000
35	2185.0000	618.0000	.0047	.0047	.0000
36	2185.0000	619.0000	.0048	.0048	.0000
37	2185.0000	620.0000	.0050	.0050	.0000
38	2185.0000	621.0000	.0051	.0051	.0000
39	2185.0000	622.0000	.0052	.0052	.0000
40	2185.0000	623.0000	.0053	.0053	.0000
41	2185.0000	624.0000	.0053	.0054	-.0001
42	2185.0000	625.0000	.0054	.0055	.0000
43	2185.0000	626.0000	.0054	.0055	-.0001
44	2185.0000	627.0000	.0055	.0055	.0000
45	2185.0000	628.0000	.0055	.0056	-.0001
46	2185.0000	629.0000	.0055	.0056	.0000
47	2185.0000	630.0000	.0055	.0056	-.0001
48	2185.0000	631.0000	.0055	.0056	-.0001
49	2185.0000	632.0000	.0054	.0055	-.0001
50	2185.0000	633.0000	.0054	.0055	-.0001
51	2185.0000	634.0000	.0053	.0054	-.0001
52	2185.0000	635.0000	.0053	.0053	.0000
53	2185.0000	636.0000	.0053	.0052	.0000
54	2185.0000	637.0000	.0051	.0051	.0000
55	2185.0000	638.0000	.0051	.0050	.0000
56	2185.0000	639.0000	.0049	.0049	.0000
57	2185.0000	640.0000	.0049	.0048	.0001
58	2185.0000	641.0000	.0046	.0046	.0000
59	2185.0000	642.0000	.0046	.0045	.0001
60	2185.0000	643.0000	.0043	.0043	.0000
61	2185.0000	644.0000	.0043	.0042	.0001
62	2185.0000	645.0000	.0040	.0040	.0000
63	2185.0000	646.0000	.0038	.0038	.0000
64	2185.0000	647.0000	.0037	.0037	.0000
65	2185.0000	648.0000	.0035	.0035	.0000
66	2185.0000	649.0000	.0034	.0033	.0001
67	2185.0000	650.0000	.0032	.0032	.0001
68	2185.0000	651.0000	.0030	.0030	.0001
69	2185.0000	652.0000	.0029	.0028	.0001
70	2185.0000	653.0000	.0028	.0027	.0001
71	2185.0000	654.0000	.0026	.0025	.0001
72	2185.0000	655.0000	.0024	.0023	.0000
73	2185.0000	656.0000	.0023	.0022	.0001
74	2185.0000	657.0000	.0021	.0020	.0000
75	2185.0000	658.0000	.0020	.0019	.0001
76	2185.0000	659.0000	.0018	.0018	.0000
77	2185.0000	660.0000	.0017	.0016	.0001
78	2185.0000	661.0000	.0015	.0015	.0000
79	2185.0000	662.0000	.0014	.0014	.0000
80	2185.0000	663.0000	.0013	.0013	.0000
81	2185.0000	664.0000	.0011	.0012	.0000
82	2185.0000	665.0000	.0011	.0011	.0000
83	2185.0000	666.0000	.0009	.0010	-.0001
84	2185.0000	667.0000	.0009	.0009	.0000
85	2185.0000	668.0000	.0007	.0008	-.0001
86	2185.0000	669.0000	.0006	.0007	-.0001
87	2185.0000	670.0000	.0006	.0007	-.0001
88	2185.0000	671.0000	.0004	.0006	-.0002
89	2185.0000	672.0000	.0004	.0005	-.0001

90	2185.0000	673.0000	.0003	.0005	-.0002
91	2185.0000	674.0000	.0003	.0004	-.0002
92	2185.0000	675.0000	.0002	.0004	-.0002
93	2185.0000	676.0000	.0001	.0004	-.0002
94	2185.0000	677.0000	.0001	.0003	-.0002
95	2185.0000	678.0000	.0000	.0003	-.0002

APPENDIX C

Discrete Sampling Method

C-1 Discrete Sampling Method

In this section, we will describe the development and testing of a new discrete sampling method, in order to allow the measurements of diffusion coefficients in high ionic strength matrices. At high ionic strengths, the signal of the eluting sample may not be distinguishable from the background signal of the matrix, and chemical separation of the sample solute from the matrix is required.

In the discrete sampling we collect outflow in sample vials for subsequent analysis by HPLC. As described below, each sample consists of one drop of sampled fluid, diluted in a larger volume of water. Discrete sampling is appropriate for chemicals/matrices of interests that cannot be monitored by an in-line detector.

Using the GC tubing as the emitter, we experimentally determined that the mean drop size was 6.8 microliters with a coefficient of variation of 2.3%. Drop intervals (depends on the flow rate, etc) in these tests had a mean of 10.53 seconds and a coefficient variation of 6.3%. These results suggest that a sample volume of 1 drop would yield adequate estimates of diffusion coefficient.

Several drop collection procedures were attempted, but most had mass

balance problems. In one procedure the single drop was collected in a sample vial, then allowed to evaporate. Subsequently, 100 microliters of water were added to the vial, the solution was mixed to insure that the sample was dissolved, and the vial placed in the autosampler of the HPLC. Although we varied this procedure we were unable to insure complete and uniform mixing of the diluted sample. A much more consistent procedure was tested and adopted, in which 100 microliters of solution was added to the vial before collection. After the drop landed in this solution, the solution was mechanically mixed using a micropipette. This insured a uniform solution, and we were unable to detect any mass loss. Samples were capped prior to running on the HPLC. 1 ml autosampler vials, 150 *u*l clear glass conical insert (max. residual volume 6 *u*l, WATO 72294) , and spring for LV1 were purchased from Waters Assoc.(Milford, MA, USA).

The final suggested discrete sampling procedure is:

1. In sample vial, add 100 μL H_2O
2. Collect 1 drop elution per vial
3. Note start time and end time
4. Mix, cap and store each sample vial
5. Run samples via HPLC
6. Convert to BTC

We also investigated other experimental details using KI as the test sample. We found a linear HPLC detector response to sample KI concentration, as shown in Figure C- 1. All HPLC analyses utilized a Waters 486 Tunable

Absorbance Detector, a Waters TM 717 Plus Autosampler , and a Waters 510 (B) HPLC Pump. Analytical column used for this work could be view in the paper of Bowman (1984a). The mobile phase used in this work was 0.1 mM potassium dihydrogen phosphate (KH_2PO_4) buffer, pH adjusted to 2.75 with 60 mM H_4PO_4, with 10 % acetonitrile as an organic modifier. The flow-rate o fthe mobile phase was 2 ml/min. The UV detector wavelength for KI is 226 nm, We injected 25 *ul* KI for each run and the rentation time of KI was 3.7 min. Analytical reproducibility was tested with typical results shown in Table C-1. Reproducibility was lower for smaller sample concentrations, suggesting that injection concentrations should be as high as possible. The trade-off is that we seek diffusion coefficients at infinite dilutions.

Table C-1 Repeatability Tests for Single Drop Samples

Concentration	Standard	Sample 1a	Sample 1b	Sample 1c
2mM	254ppm	255	256	256
1mM	127	129	129	129
0.5mM	63.5	65.2	64.7	64.0
0.1mM	12.7	16.3	16.0	14.9

Finally we ran a diffusion experiment through the tubing while sampling both continuously and discretely (file PH17Aug.01l). We injected 20mM KI to insure a better record of discrete breakthrough, which is shown in Figure C -2. The diffusion coefficient measured by discrete sampling was $1.89 \times 10^{-9}\ m^2s^{-1}$. Unfortunately we failed to reset the inline detector (Waters lambda – Max Model

481 LC spectrophotometer) so that the peak part of the breakthrough was off-scale. Without a peak to scale the results, the continuous record cannot be compared to the discrete record shown in the figure. Later we changed to the capillary detector described in the main text and measured a diffusion coefficient for 20 mM KI by continuous sampling, and recorded it as $1.86 \times 10^{-9}\ m^2s^{-1}$. It suggests that there was less dispersion resulting from the discrete sampling method.

C-2 Effect of drop size on diffusion coefficients

In addition to conducting physical experiments, which use an inline detector for continuous monitoring of concentration, we have simulated the effect of using a fraction collector to acquire discrete samples. The purpose of this simulation was to determine the maximum sample size that would produce reliable results using the current method.

On both plots in Figure C-3, the Gaussian curve depicts real data acquired at one-second intervals. The curve shown here is one of the dispersion profile recorded at 0.5 ml/min. On vertical axis is the signal from an ultraviolet detector, which is representative of solute concentration. To remove noise outside the elution curve, values below 10^4 *u*V have been eliminated. The bars indicate simulated concentrations averaged over 20 *u*l in the first graph and 50 *u*l in the second graph. Each bar can be thought of as a vial in a fraction collector, where the concentration is averaged over a short period of time.

As the fraction size increases, the error in measuring the diffusion coefficient also increases. Figure C-4 shows the absolute value of diffusion coefficient measurement error increasing with fraction size. The lowest point on the graph shows the actual error (0.19%) from the experimental data. The experimental data were recorded at one-second intervals with a flow rate of 0.05 ml/min, represented here as a sample size of 0.83 *u*l.

Future work will include determining the smallest practicable fraction size. We are also looking at ways to increase the elution volume (the volume of fluid containing solute) by methods such as increasing the tube length or decreasing the flow rate. Clearly, a high ratio of elution volume to fraction size would be beneficial in getting an accurate representation of the elution curve using fraction collection. Further development of the software, as described above, will also lead to more accurate measurements for both continuous and discrete samling.

Based on the results to date, it appears that the method will be capable of making the desired measurements, at least for chemicals that can be detected in-line. Although our analysis of fraction collection is still preliminary, indications are that we will be able to make measurements that are within an accuracy range of 10%.

C-3 Current Issues

There are a series of current issues that we are still working on. Although we outline the sample collection and mixing procedure above, we are still seeking ways to improve it. In particular we seek a better way to mix the samples than using a micropipette. Timing of the injection and breakthrough is still based

on hand and eye coordination, and can be improved. To achieve results for diffusion coefficients representing infinite dilution we need to reduce the injection concentration to 2mM, and need to improve the procedure so that we can get repeatable results in this concentration range. The technique produces results with a greater standard deviation and bias than desired; we need to continue to improve and practice procedure. Finally, we need to further test measurement of diffusion coefficients using the discrete sampling method, especially with a brine matrix.

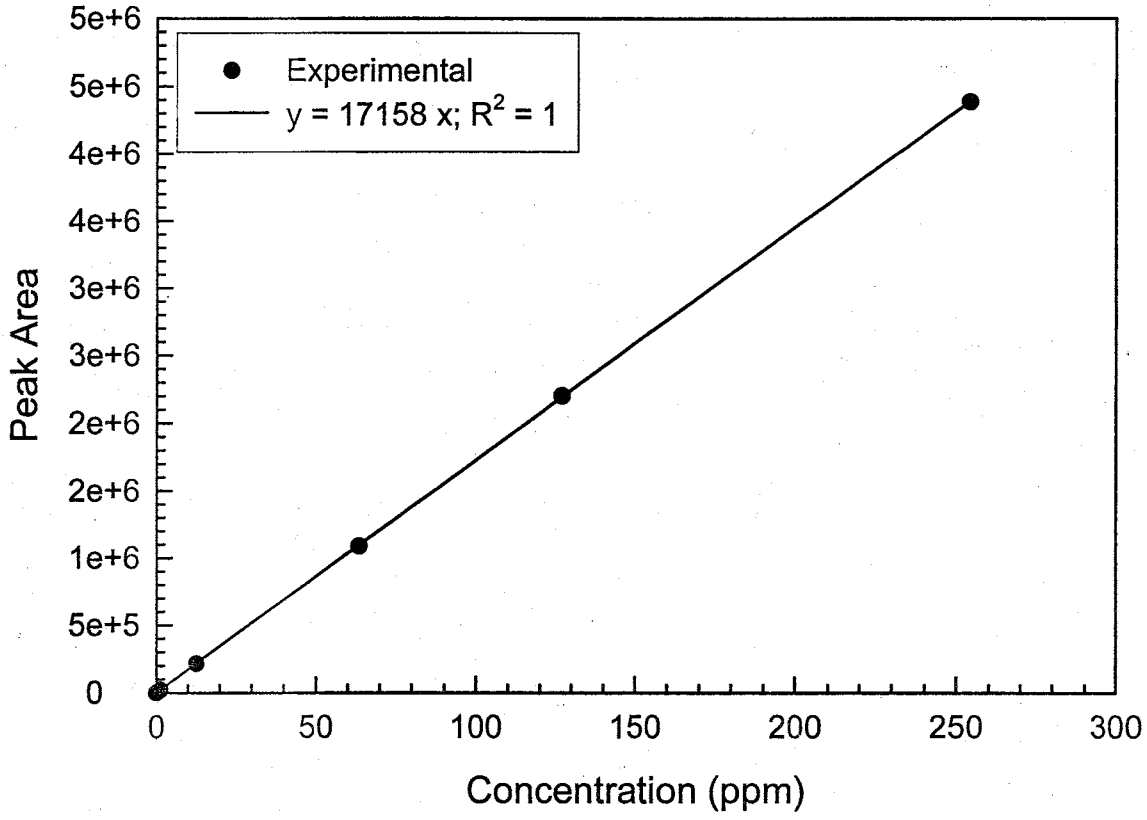

Figure C-1 Calibration curve for KI measured by HPLC system

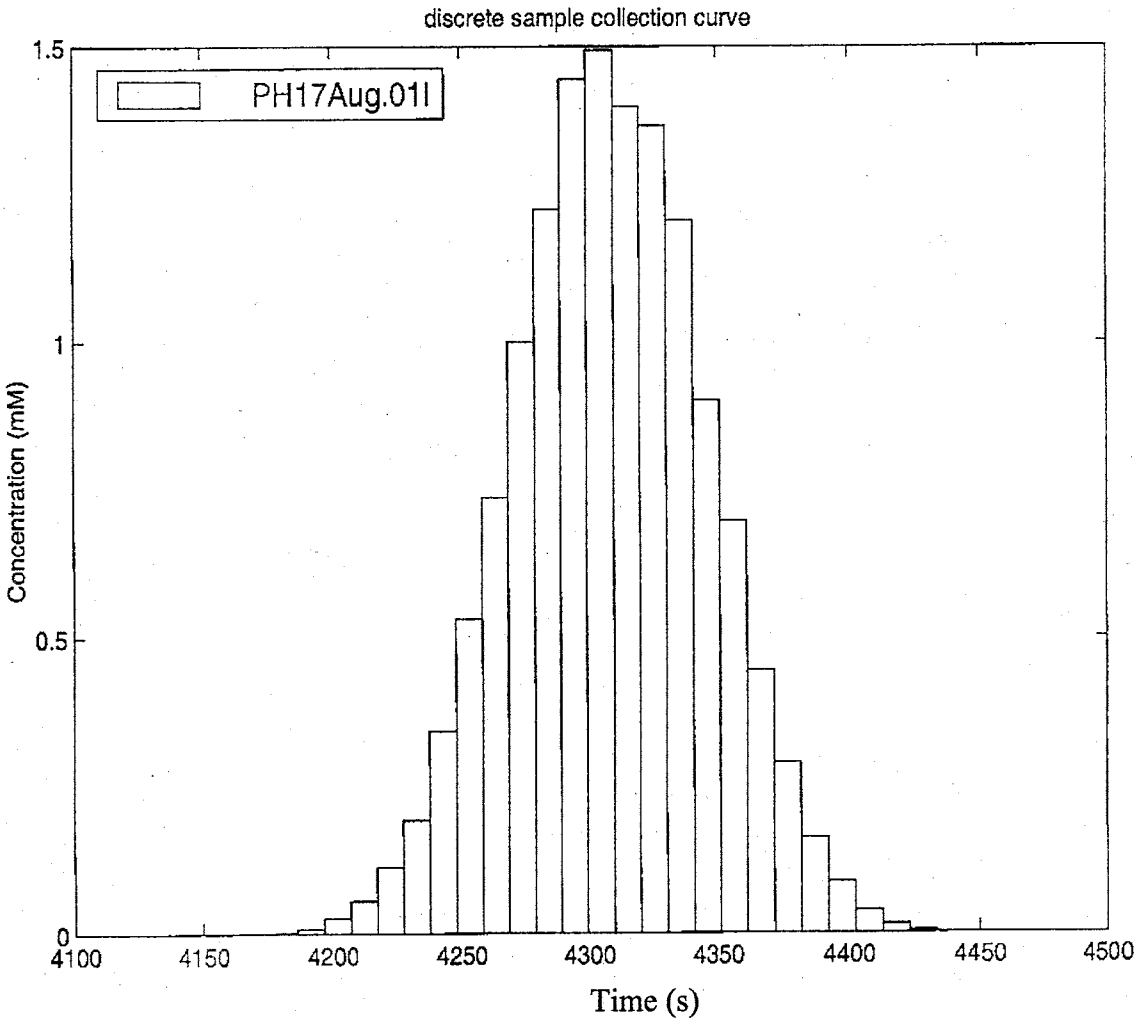

Figure C-2 Discrete sampling breakthrough curve

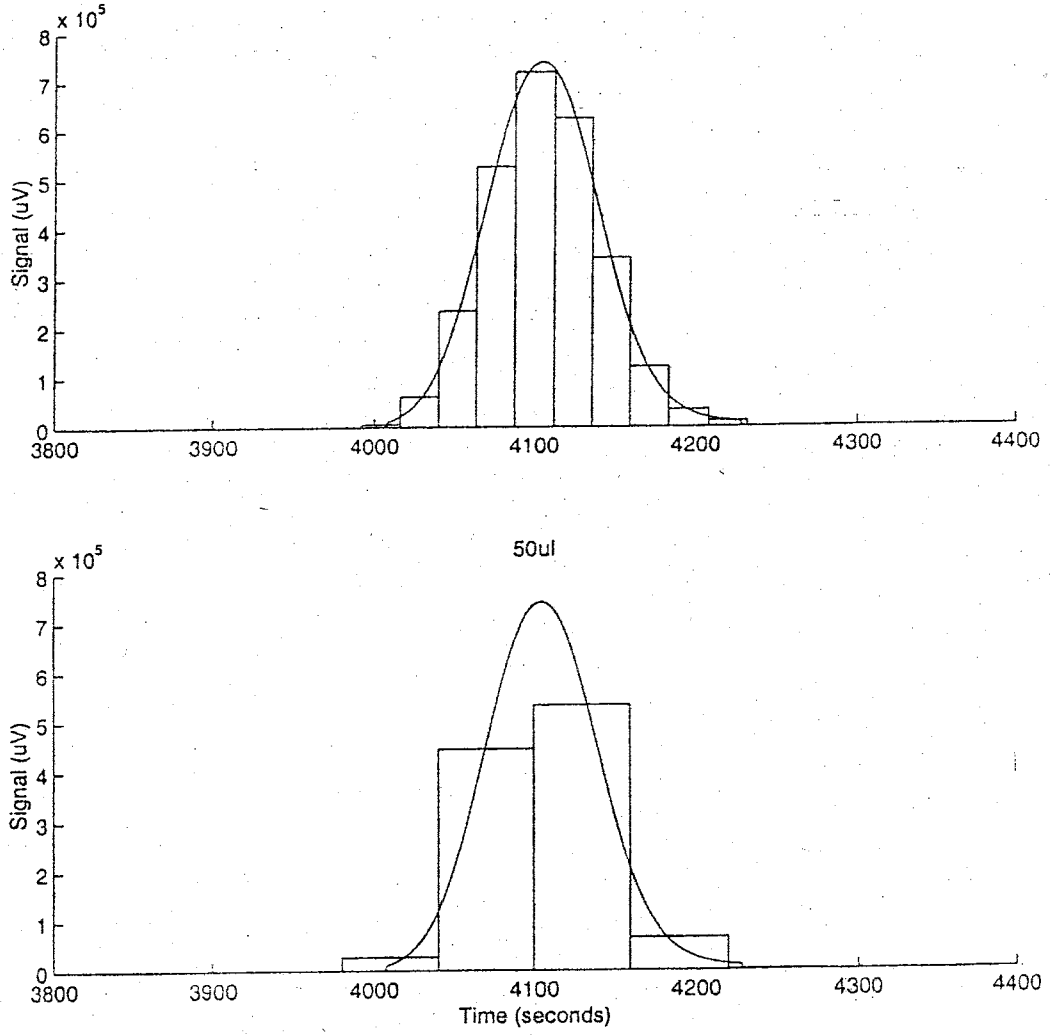

Figure C-3 Simulated fraction collection

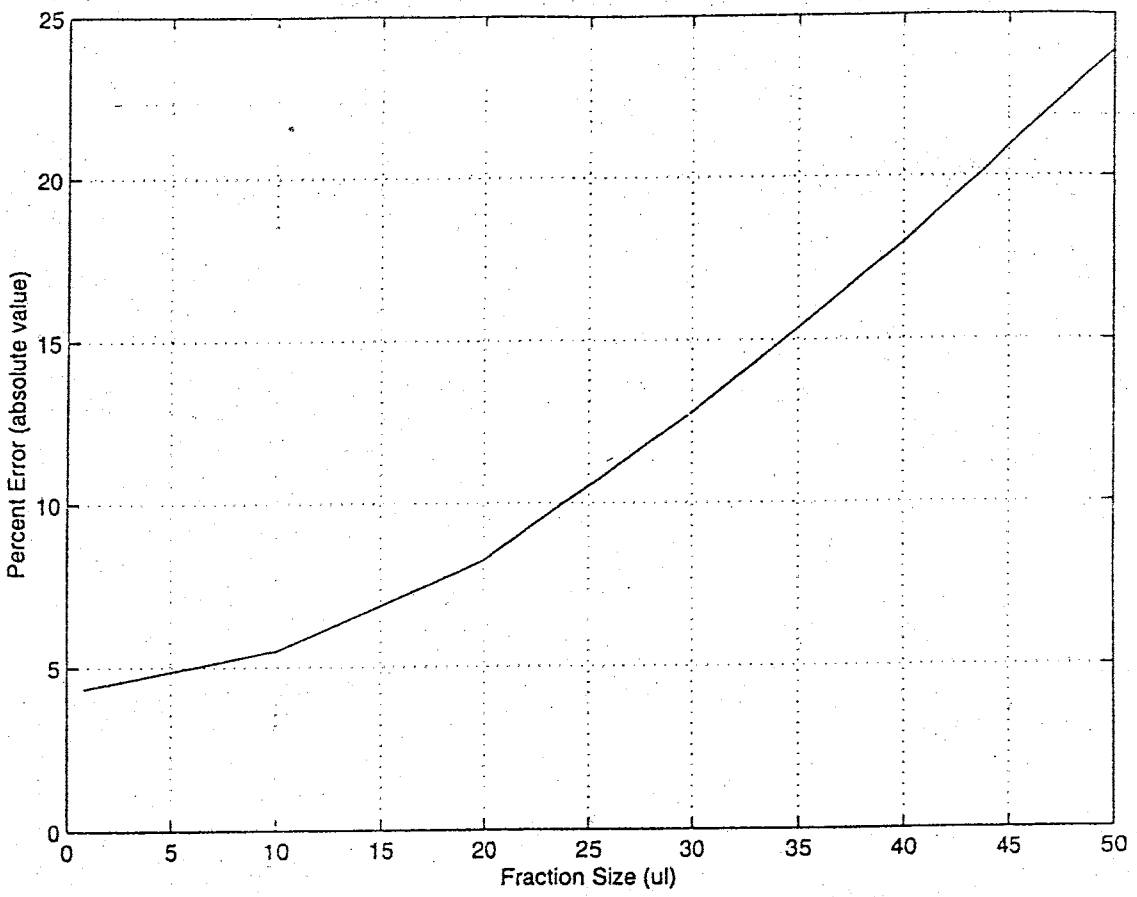

Figure C-4 Magnitude of Error as a function of fraction size

APPENDIX D

Flow Rate – Dependent Diffusion

We measured diffusion coefficients of KCl, KBr, and KI in water at different flow rates of injection. The diffusion coefficient data of KCl, KBr, and KI at different results at the flow rates of 0.01, 0.05, and 0.1 ml/min are given in Table D-1. Again, different detector wavelengths are used for KCl, KBr, and KI in order to maximize the sensitivity during diffusion coefficient measurements. Figure D-1 shows the diffusion coefficient of KCl (A), KBr (B), and KI (C) at different initial concentrations versus flow rates. These results show a consistent pattern for the same compound at the same concentration, with the diffusion coefficients increasing slightly with increasing flow rates. This observation conflicts with a general concept that diffusion is the instrinsic property of a molecule, and the diffusion coefficient should not be dependent on the flow rate. In fact, we are not yet able to give a proper explanation as to why the diffusion coefficient changes with the flow rate. However, we noticed that the error of each measurement could be up to about 5 percent, thus, the change of the diffusion coefficient with the flow rates for the same compound at the same concentration is indeed marginal.

Table D-1 Diffusion coefficients of KCl, KBr, and KI in water at different flow rates

Chemicals	Concentration (mM)	Flow rate (ml/min)	Diffusion coefficient ($m^2s^{-1} \times 10^{-9}$)	Detector Wavelength (nm)
KCl	20	0.05	1.90	190
		0.10	1.90	
	50	0.05	1.79	
		0.10	1.85	
	100	0.05	1.67	
		0.10	1.76	
	200	0.05	1.56	
		0.10	1.67	
KBr	2	0.01	1.87	208
		0.05	1.93	
		0.10	1.97	
KI	0.5	0.05	1.92	226
		0.10	1.97	
	1	0.05	1.91	
		0.10	1.94	
	2	0.05	1.91	
		0.10	1.91	
	10	0.05	1.87	
		0.10	1.89	
	20	0.05	1.86	
		0.10	1.87	

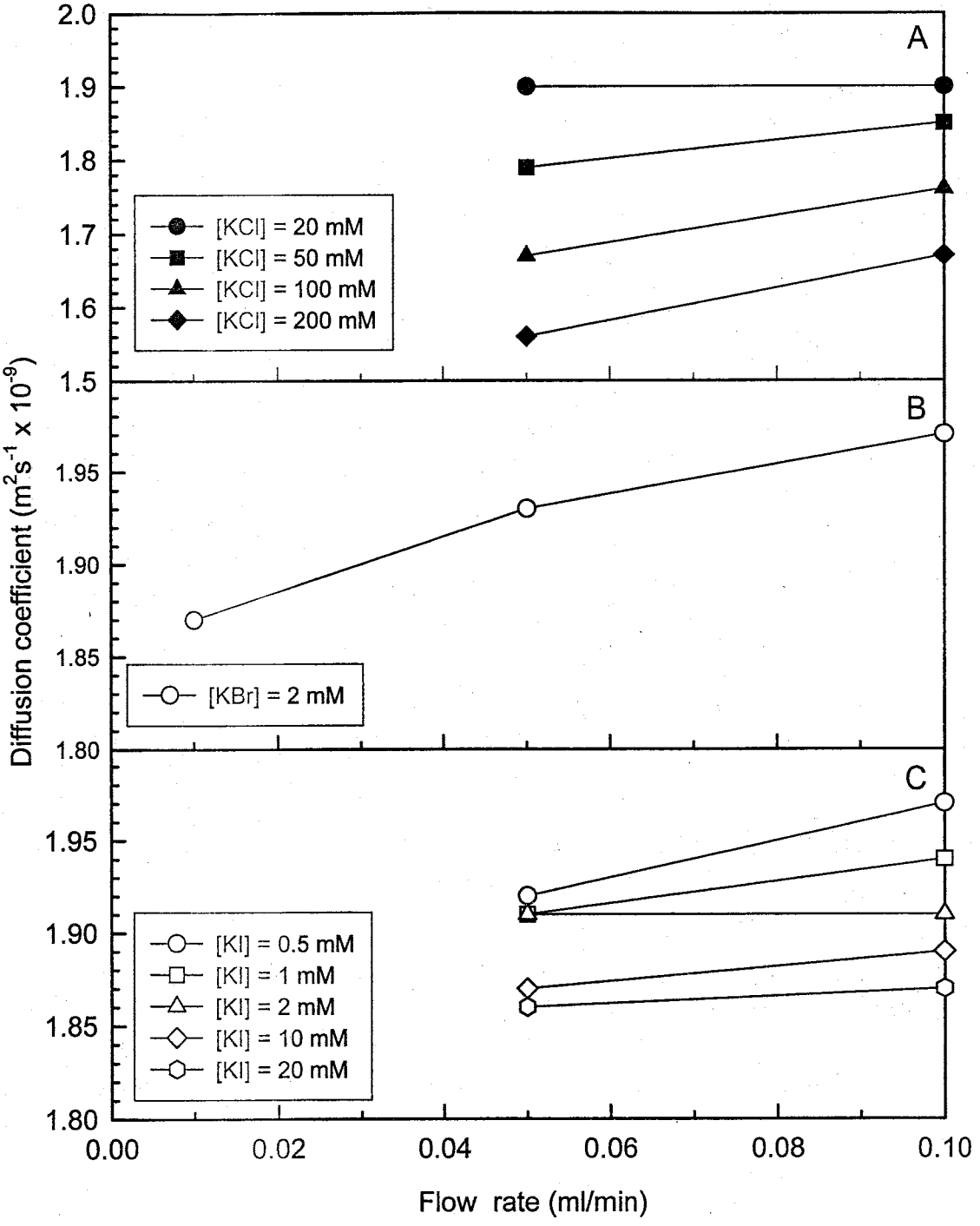

Figure D-1 Diffusion coefficients of KCl (A), KBr (B), and KI (C) in water versus the flow rates of injection

APPENDIX E

Statistical Analysis of Variance for Raw Diffusion Coefficient Data

The raw diffusion coefficient data of FBAs and CBAs in both water and a buffer solution are summarized in Table E-1. In order to investigate the change in mean diffusion coefficients of FBAs either with the same molecule weight or with different molecular weights, we performed both a one-way and two-way analysis of variance (ANOVA). To perform this analysis, we first prepared an input file of the raw diffusion coefficient data, and then we used the MINITAB (version 13) software program. The analysis results for FBAs and DCBAs in both water and a buffer solution are given below:

One-way ANOVA for Compounds in Water

One-way ANOVA was performed for compounds in water (E-1) to investigate the change in mean diffusion coefficients of FBAs in water.

For the FBAs of different molecular weights, there is no statistically significant difference in the mean diffusion coefficients for PFBA, TFBA, and DFBA. Similarly, there is no statistically significant difference in the mean diffusion coefficients for TFMBA, TeFBA, and DCBA. However, the mean diffusion coefficients for PFBA, TFBA and DFBA are relatively larger than that for the other three groups.

For the FBAs within each group having the same molecular weight, there is some difference in diffusion coefficients for those compounds with the same molecular weight. For DFBAs in water, there is no statistically significant difference in the mean diffusion coefficient for 2,4 DFBA, 2,5 DFBA and 3,4 DFBA. Similarly, there is no statistically significant difference in the mean diffusion coefficient for 2,6 DFBA and 3,5 DFBA. However, the mean diffusion coefficient for 2,3 DFBA is relatively larger than that for 2,4 DFBA, 2,5 DFBA and 3,4 DFBA, followed by the other two compounds.

There is no statistically significant difference in the mean diffusion coefficient for compounds within the following groups, each having the same molecular weight: five TFBAs, two DCBAs and two TFMBAs.

There is a significant difference in the mean diffusion coefficient for 2,3,4,5 TeFBA and 2,3,5,6 TeFBA.

One-Way ANOVA for Compounds in Buffer Solution

For compounds in buffer solution (output E-2), we used one-way ANOVA to investigate the change in mean diffusion coefficients of compounds in a buffer solution.

For the FBAs of different molecular weights, there is no statistically significant difference in the mean diffusion coefficients for TeFBA, TFBA, DCBA and DFBA. Similarly, there is no statistically significant difference in the mean diffusion coefficients for TFMBA and PFBA. However, the mean diffusion

coefficients for TeFBA, TFBA, DCBA and DFBA are relatively larger than that for the other two groups.

For the FBAs within each group having the same molecular weight, there is some difference in diffusion coefficients with the same molecular weight. For DFBAs in buffer solution, there is no statistically significance difference in the mean diffusion coefficient for 2,3 DFBA, 2,4 DFBA, 2,5 DFBA and 2,6 DFBA. Similarly, there is no statistically significant difference in the mean diffusion coefficient for 3,4 DFBA and 3,5 DFBA. However, the mean diffusion coefficients for 2,3 DFBA, 2,4 DFBA, 2,5 DFBA and 2,6 DFBA are relatively larger than that for the other two compounds.

In addition, there is no statistically significant difference in the mean diffusion coefficient for compounds with the same molecular weight for the five TFBAs, two TeFBAs, two DCBAs and two TFMBAs.

Two-Way ANOVA on Water and Buffer Solutions

A two-way ANOVA (output E-3) was used to investigate the change in mean diffusion coefficients of FBAs and DCBAs in both water and a buffer solute. In table C3 is the diffusion coefficient measured, C2 is the name of the compound, and C1 indicates the solution condition, water or buffered. C3 responded to both C1 and C2. In other words, the change in diffusion coefficient depends on the compounds and medium condition.

All three effects are statistically significant. The medium effect (- water or buffer) has the largest F statistic (74.84), followed by the compound species

effect (F value = 7.72) and the compounds-by-medium interaction (F value = 3.25).

The difference in mean diffusion coefficient between the water and buffer solution varies for different compounds.

If we ignore the compounds-by-medium interaction for the FBAs of different molecular weights, there is no statistically significant difference in the mean diffusion coefficients for TFBA and DFBA. Similarly, there is no statistically significant difference in the mean diffusion coefficients for TFMBA, TeFBA, DCBA and PFBA. However, the mean diffusion coefficients for TFBA and DFBA are relatively larger than that for the other four groups.

For the FBAs within each group having the same molecular weight, there is no statistically significant difference in the mean diffusion coefficients.

Thus, the differences in diffusion coefficients for compounds either with the same molecular weight or with a different molecular weight are larger in water than in the buffer solution. However, the interpretation of the diffusion coefficients in water is complicated by the fact that different FBAs have different ratios of neutral to anionic form.

Table E-1 Raw **diffusion coefficient data of FBAs and CFBAs in both water and a buffer solution**

Chemicals	Diffusion coefficient ($m^2s^{-1} \times 10^{-9}$)					
	In water			In potassium phosphate buffer		
	Run 1	Run 2	Run 3	Run 1	Run 2	Run 3
Benzoic acid	0.98	0.96		0.89	1.01	0.93
2,3 DFBA	1.00	0.99	0.95	0.94	0.91	0.96
2,4 DFBA	0.94	0.96	0.89	0.92	0.89	0.93
2,5 DFBA	0.96	0.96	0.94	0.97	0.94	0.92
2,6 DFBA	0.88	0.87		0.95	0.92	0.98
3,4 DFBA	0.94	0.97	0.94	0.83	0.80	0.84
3,5 DFBA	0.91	0.91	0.95	0.88	0.84	
2,3,4 TFBA	0.97	0.93	0.91	0.92	0.92	
2,3,6 TFBA	0.98	0.94	0.94	0.81	0.81	0.86
2,4,5 TFBA	0.93	0.93	0.96	0.81	0.83	
2,4,6 TFBA	0.92	0.97		0.87	0.82	0.83
3,4,5 TFBA	0.96	0.95	0.93	0.93	0.86	0.83
2,3,4,5 TeFBA	0.93	0.94	0.97	0.87	0.91	0.88
2,3,5,6 TeFBA	0.86	0.84		0.84	0.77	0.81
PFBA	0.92	0.94		0.75	0.73	
m-TFMBA	0.89	0.88	0.87	0.72	0.85	0.79
o-TFMBA	0.85	0.86	0.86	0.76	0.85	
2,4 DCBA	0.87	0.88	0.93	0.78	0.85	
3,5 DCBA	0.87	0.87	0.86	0.90	0.83	

12/6/00 9:18:14 PM

Welcome to Minitab, press F1 for help.

One-way ANOVA: C3 versus C4

Analysis of Variance for C3

Source	DF	SS	MS	F	P
C4	6	0.03971	0.00662	6.53	0.000
Error	31	0.03140	0.00101		
Total	37	0.07111			

Level	N	Mean	StDev
benz	2	0.9700	0.0141
dcba	4	0.8725	0.0050
dfba	12	0.9408	0.0410
pfba	2	0.9300	0.0141
tefba	4	0.8925	0.0499
tfba	10	0.9480	0.0210
tfmbam	4	0.8700	0.0183

Pooled StDev = 0.0318

Individual 95% CIs For Mean
Based on Pooled StDev

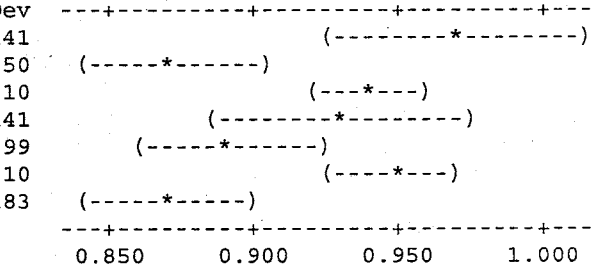

One-way ANOVA: C3 versus C2

Analysis of Variance for C3

Source	DF	SS	MS	F	P
C2	18	0.066658	0.003703	15.81	0.000
Error	19	0.004450	0.000234		
Total	37	0.071108			

Level	N	Mean	StDev
benz	2	0.9700	0.0141
dcba24	2	0.8750	0.0071
dcba35	2	0.8700	0.0000
dfba23	2	0.9950	0.0071
dfba24	2	0.9500	0.0141
dfba25	2	0.9600	0.0000
dfba26	2	0.8750	0.0071
dfba34	2	0.9550	0.0212
dfba35	2	0.9100	0.0000
pfba	2	0.9300	0.0141
tefba234	2	0.9350	0.0071
tefba235	2	0.8500	0.0141
tfba234	2	0.9500	0.0283
tfba236	2	0.9600	0.0283
tfba245	2	0.9300	0.0000
tfba246	2	0.9450	0.0354
tfba345	2	0.9550	0.0071
tfmbam	2	0.8850	0.0071
tfmbao	2	0.8550	0.0071

Pooled StDev = 0.0153

Individual 95% CIs For Mean
Based on Pooled StDev

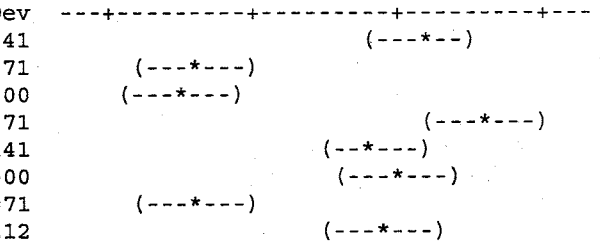

E-2 Compounds In Buffer Solution

One-way ANOVA: C7 versus C4

```
Analysis of Variance for C7
Source      DF        SS         MS        F        P
C4           6   0.08257    0.01376     4.70    0.002
Error       31   0.09083    0.00293
Total       37   0.17340

                                        Individual 95% CIs For Mean
                                        Based on Pooled StDev
Level       N      Mean     StDev  ----+---------+---------+---------+--
benz        2    0.9500    0.0849                      (-------*-------)
dcba        4    0.8400    0.0497             (-----*-----)
dfba       12    0.8992    0.0526                      (--*--)
pfba        2    0.7400    0.0141  (-------*-------)
tefba       4    0.8475    0.0591               (-----*----)
tfba       10    0.8580    0.0496                  (---*--)
tfmbam      4    0.7950    0.0656          (----*-----)
                                        ----+---------+---------+---------+--
Pooled StDev =    0.0541                  0.70      0.80      0.90      1.00
```

One-way ANOVA: C7 versus C6

```
Analysis of Variance for C7
Source      DF        SS         MS        F        P
C6          18   0.13840    0.00769     4.17    0.002
Error       19   0.03500    0.00184
Total       37   0.17340

                                        Individual 95% CIs For Mean
                                        Based on Pooled StDev
Level       N      Mean     StDev  ---+---------+---------+---------+---
benz        2    0.9500    0.0849                        (-----*-----)
dcba24      2    0.8150    0.0495          (-----*------)
dcba35      2    0.8650    0.0495               (-----*------)
dfba23      2    0.9250    0.0212                    (------*-----)
dfba24      2    0.9050    0.0212                 (------*-----)
dfba25      2    0.9550    0.0212                      (-----*------)
dfba26      2    0.9350    0.0212                   (------*-----)
dfba34      2    0.8150    0.0212          (-----*------)
dfba35      2    0.8600    0.0283               (-----*-----)
pfba        2    0.7400    0.0141   (-----*-----)
tefba234    2    0.8900    0.0283                    (-----*-----)
tefba235    2    0.8050    0.0495         (-----*------)
tfba234     2    0.9200    0.0000                   (-----*-----)
tfba236     2    0.8100    0.0000          (-----*-----)
tfba245     2    0.8200    0.0141           (-----*-----)
tfba246     2    0.8450    0.0354             (-----*------)
tfba345     2    0.8950    0.0495                  (-----*------)
tfmbam      2    0.7850    0.0919       (-----*------)
tfmbao      2    0.8050    0.0636         (-----*------)
                                        ---+---------+---------+---------+---
Pooled StDev =    0.0429                 0.70      0.80      0.90      1.00
```

E-3 Compounds analysis ignore the medium condition

12/6/00 1:39:26 PM

Two-way ANOVA: C3 versus C2, C1

```
Analysis of Variance for C3
Source        DF        SS        MS        F        P
C2            18   0.14433   0.00802     7.72    0.000
C1             1   0.07770   0.07770    74.84    0.000
Interaction   18   0.06073   0.00337     3.25    0.001
Error         38   0.03945   0.00104
Total         75   0.32220
```

Residuals vs Fits for C3

Residuals vs Order for C3

One-way ANOVA: C3 versus C2

```
Analysis of Variance for C3
Source     DF        SS        MS        F        P
C2          6   0.11364   0.01894     6.36    0.000
Error      95   0.28270   0.00298
Total     101   0.39633

                                    Individual 95% CIs For Mean
                                    Based on Pooled StDev
Level      N      Mean     StDev  ----------+---------+---------+------
benz       5    0.9540    0.0462                      (-------*-------)
dcba      10    0.8640    0.0401           (-----*-----)
dfba      34    0.9229    0.0475                      (--*--)
pfba       4    0.8350    0.1103  (--------*--------)
tefba     11    0.8745    0.0596             (-----*----)
tfba      27    0.9007    0.0570                   (--*---)
tfmba     11    0.8345    0.0539      (----*-----)
                                    ----------+---------+---------+------
Pooled StDev =    0.0546                  0.840     0.900     0.960
```

Two-way ANOVA: C3 versus C2, C1

```
Analysis of Variance for C3
Source        DF        SS        MS        F        P
C2            18   0.14433   0.00802     4.48    0.000
C1             1   0.07770   0.07770    43.43    0.000
Error         56   0.10018   0.00179
Total         75   0.32220
```

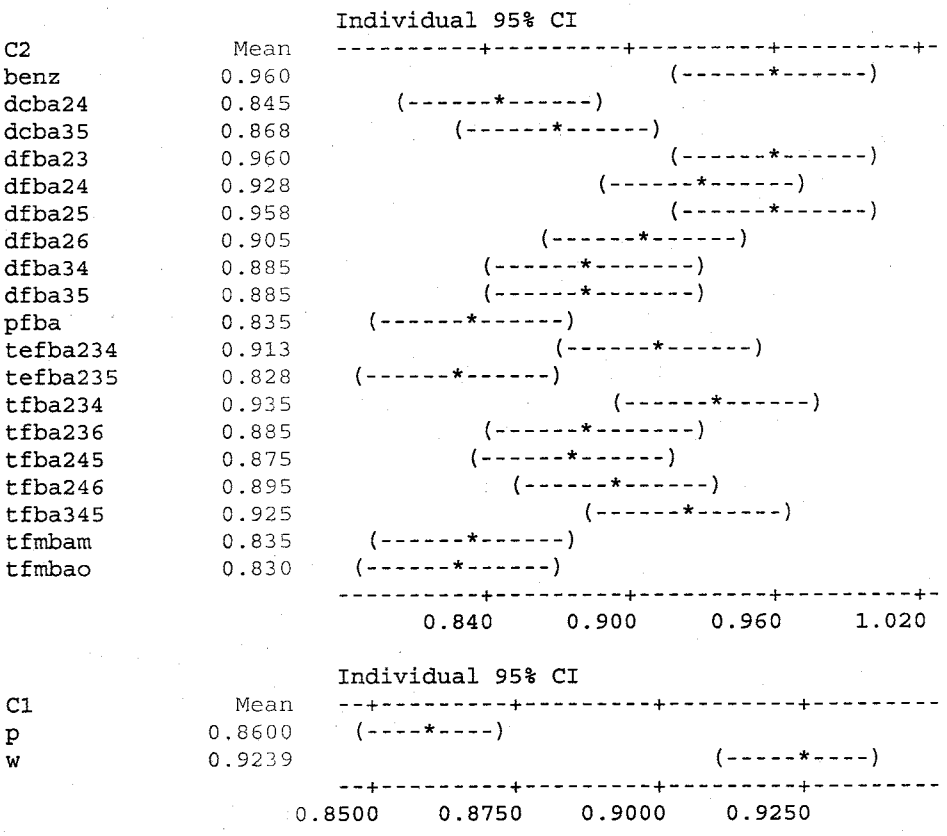

Residuals vs Fits for C3

Residuals vs Order for C3

```
Saving file as: C:\WINDOWS\DESKTOP\ping1.MPJ
```

APPENDIX F

Diffusion Coefficients of Two Dye Tracers: Uranine and Brilliant Blue FCF

We completed the development of an experimental system for measuring diffusion coefficients of hydrologic tracers and measured the diffusion coefficients of 18 FBAs and DCBAs tracers. Currently, dye tracing techniques are widely used in hydrology. Due to lack of diffusion coefficients for dye tracers, we applied our experimental system to measure the diffusion coefficients of uranine (also known as fluorescein) and brilliant blue FCF (also known as FD&C blue #1). We carried out four measurements for each compound. The average diffusion coefficient data of each dye tracer is given in Table F-1. The diffusion coefficient data of hydrologic tracers are very fundamental parameters for the evaluation of the flow and transport process under saturated zones.

Table F-1 Diffusion coefficients of Uranine and Brilliant Blue FCF in water

Chemicals	Concentration (mM)	Detector Wavelength (nm)	Mean diffusion coefficient ($m^2s^{-1}x10^{-9}$)	Standard deviation
Uranine	0.1	320	0.615	0.017
	0.3	320	0.648	0.005
Billiant Blue FCF	0.1	308	0.568	0.01

APPENDIX G

Tube Radius Measurement

We estimated the tube radius using three independent methods: a pressure-differential method, a microscopy method, and a gravimetric method

G-1 Pressure-differential method

In the pressure–differential method, we installed a differential pressure transducer at the beginning of the diffusion tube and used the pressure transducer to record the maximum pressure drop. The pressure at the end of the tube was assumed to be atmospheric (capillary effects during the formation of drops was negligible). By Poiseuille's Law, the flow rate through a capillary in terms of pressure drop, ΔP, is given by:

$$Q = \frac{\pi R^4}{8} \frac{1}{\mu} \frac{\Delta P}{L} \qquad \text{(G.1)}$$

where Q is the flow rate of solution and μ is the viscosity of the solution. The tube radius was measured repeatedly at several different flow rates (Table G-1). The average tube radius was calculated to be 122 ± 3 μm, with a standard deviation 0f 3 μm.

Table G-1 Tube radius measurements at different flow rates

Flow rate (ml/min)	Pressure (psi)	Tube length (cm)	Viscosity ($Pa.sx10^{-3}$)	Calculated tube radius (cm)
0.027	18.1	2531	0.8937	0.012050
0.044	29.7	2531	0.8937	0.011996
0.094	58.7	2531	0.8937	0.012231
0.115	70.7	2531	0.8937	0.012279
0.143	88.6	2531	0.8937	0.012255
0.189	118.5	2531	0.8937	0.012219
0.241	148.0	2531	0.8937	0.012283

G-2 Optical method

In the optical method, we randomly cut the capillary tube and observed its cross-sectional area under optical microscopy and SEM (Figure G-1). The tube radius was measured eight times by a Scion image software program and averaged to be 120 ± 3 μm. This method was not really accurate because the shape of the tube was altered by hand cutting.

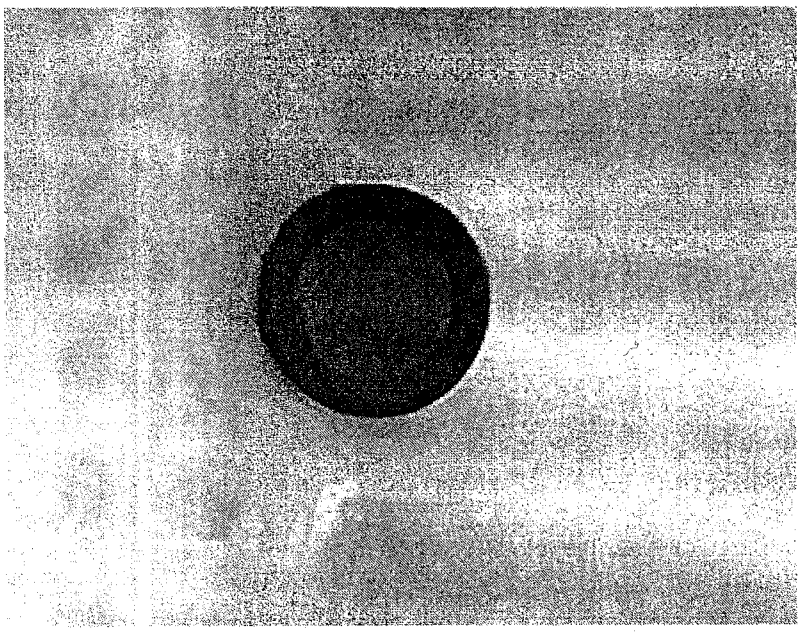

Figure G-1 Image tube cross-section under optical microscopy (100x1)

G-3 Gravimetric method

In the gravimetric method, we randomly selected tubes of different lengths and weighed each tube when it was empty and when filled with mercury of known density. We measured the mass of mercury in the tube, and then converted that to the volume of mercury and then to the tube radius. The results are shown in Table G-2. The density of mercury is 13.6 g/ml at 25^0 C. The average tube radius was determined to be 124 $\pm$ 1 μm. This method was more accurate than the optical method. However, the longest tube for measurements using this method was 1 meter. This result does not necessarily represent the average radius of the 2185 cm long tube used in the experiment.

Table G-2 Tube radius **measurements based on the gravimetric method.**

Mercury weight (mg)	Length of mercury in tube (cm)	Calculated tube radius (cm)
18.2	2.80	0.0124
24.0	3.60	0.0125
28.0	4.40	0.0124
36.6	5.70	0.0123
58.6	9.05	0.0123
72.2	11.10	0.0124

The values for the tube radius measured by the above three methods were in good agreement, and were also close to the radius (125 ± 6 μm) of this small bore capillary tube cited by the manufacturer. However, we believe that the pressure-differential method provides the most accurate estimate because it represents the average tube radius of the entire tube used in the experiments, while the others do not. We used this result (tube radius =122 ± 3 μm) to calculate the diffusion coefficient based on equation (2.13).

APPENDIX H

The Standard Calibration Curves of Tracers

A standard calibration curve was made for some tracers in water. We can disconnect tube from the mobile phase reservoir and then continuously injected tracers (at low concentrations) into our experimental system and waited until the voltage readings were constant. This constant value was used as the voltage for the data of the calibration curve. By injecting the different concentrations of tracers, we could build the calibration curves. Figure H-1 demonstrated that the voltage (the analog signal) was proportional to the solute concentration. The dispersion coefficient was calculated from the concentration profiles generated by the solute dispersion curve using the CXTFIT2 model. The calibration concentration was the same as the concentration injected for the diffusion coefficient determination.

For other tracers either in water or a potassium phosphate buffer solution, we did not make the calibration curves. Instead, we continuously injected tracer samples into the experimental system and recorded the constant voltage readings. These constant values were used as the input concentration parameter in the CXTFIT 2 model. At that time, the solute dispersion curve did not need to be converted to the concentration profile based on the calibration curve. The

dispersion coefficients were calculated from the solute dispersion curve using the CXTFIT2 model. These two methods(making or not making calibration curves) would not change the diffusion coefficient values.

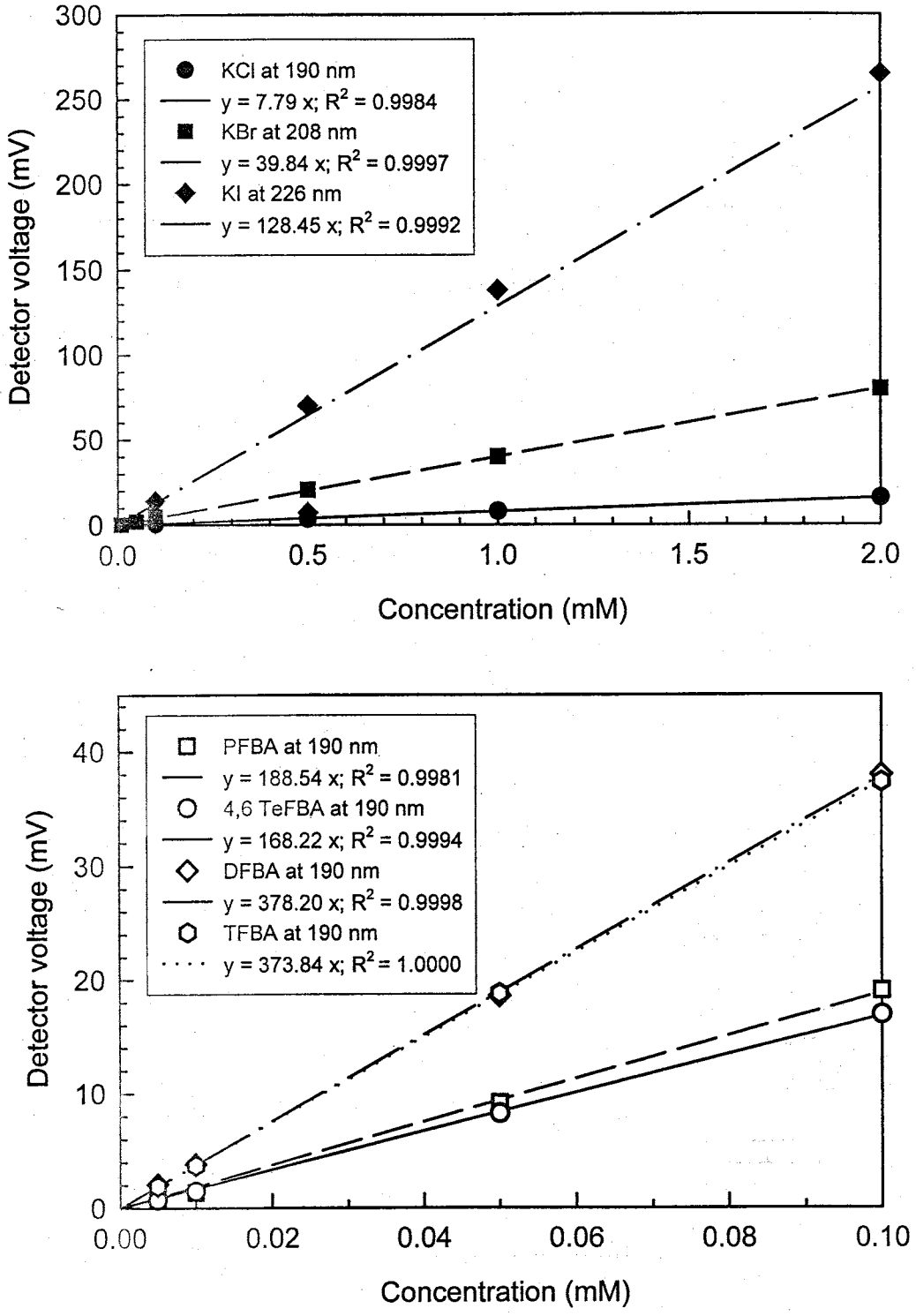

Figure H-1 Calibration **curves of tracers at different wavelengths**